NASA CONTRACTOR
REPORT

NASA CR-1335

TURBULENCE IN THE MIXING REGION BETWEEN DUCTED COAXIAL STREAMS

by J. J. Leithem, R. A. Kulik, and H. Weinstein

Prepared by
ILLINOIS INSTITUTE OF TECHNOLOGY
Chicago, Ill.
for Lewis Research Center

NATIONAL AERONAUTICS AND SPACE ADMINISTRATION • WASHINGTON, D. C. • JULY 1969

NASA CR-1335

TURBULENCE IN THE MIXING REGION BETWEEN DUCTED COAXIAL STREAMS

By J. J. Leithem, R. A. Kulik, and H. Weinstein

Prepared under Grant No. NsG-694SC by
ILLINOIS INSTITUTE OF TECHNOLOGY
Chicago, Ill.

for Lewis Research Center

NATIONAL AERONAUTICS AND SPACE ADMINISTRATION

For sale by the Clearinghouse for Federal Scientific and Technical Information
Springfield, Virginia 22151 – CFSTI price $3.00

ABSTRACT

An experimental investigation of both homogeneous and heterogeneous compound ducted jets is presented for axially symmetric coflowing streams. The flow system considered in one of a circular 3 inch inner stream issuing into a circular 6 inch, faster moving, outer stream. Air was used for the outer stream gas and both air and Freon-12 were used for the inner jet. This gave density ratios of 1 and 4, inner to outer stream, respectively. The velocity ratio was varied from 4.19 to 30.0 for both cases, with absolute velocities of 1.5 to 40 ft/sec.

All data were taken with a constant temperature hot wire anemometer system. Average velocity, radial and axial turbulence intensity profiles both near and far downstream are presented for the homogeneous cases. Average velocity, density and axial turbulence intensity profiles as well as mass holdup data both near and far downstream are presented for the heterogeneous cases.

The ratio of axial to radial turbulence intensity was about 1.5, the same as found for unconfined coaxial flow. For the higher density ratio cases, the inner stream integrity was maintained better than for the homogeneous cases. The flow system was found to be one of combined wake-coaxial flow with possible backflow.

Data for this case consist of average velocity and concentration profiles, axial turbulence intensity profiles, and mass holdup profiles.

FOREWORD

Research related to advanced nuclear rocket propulsion is described herein. This work was performed under NASA Grant NsG-694SC with Mr. Maynard F. Taylor, Nuclear Systems Division, NASA Lewis Research Center as Technical Manager.

TABLE OF CONTENTS

LIST OF SYMBOLS

Symbol	Definition
A	A constant in the hot wire anemometer equation
B	A constant in the hot wire anemometer equation
R	Resistance of sensor
z	Axial coordinate
u	Component of velocity in direction of flow field
v	Component of velocity perpendicular to flow field
U_o	Maximum outer stream velocity at zero axial position
V	Normal velocity past the sensor
T	Temperature
P	Power input to sensor
P_c	Power input to aspirator probe
A_t	Eddy viscosity
N_u	Nusselt Number
P_r	Prandtl Number
R_e	Reynolds Number
t	Time
r	Radius - distance from centerline of center tube
r_o	Radius of inner tube
d	Diameter of sensor
l	Length of sensor
k	Thermal Conductivity
e	Conversion constant

List of Symbols - cont.

Greek Symbols	
ρ	Density
τ_{zr}	Laminar shear stress
τ^{t}_{zr}	Turbulent shear stress
μ	Molecular viscosity
α	Coefficient of electrical resistivity

Superscripts	
—	Time average
'	Fluctuating component

Subscripts	
1	Refers to sensor 1
2	Refers to sensor 2

INTRODUCTION

The topic of the mixing of two coaxially flowing gaseous streams has become one of increased importance in recent years. The development of such devices as ejectors, jet pumps and combustion chambers, and more recently, the gaseous core nuclear rocket has sounded the need for further research on the subject. Current investigations may be categorized into groups depending on the particular physical characteristics of the flow system under investigation. The flow of the two streams may be parallel or countercurrent, laminar or turbulent. The jet is termed heterogeneous if it is composed of two dissimilar fluid streams and homogeneous if the two fluids are similar or the same. In addition, the outer stream may or may not be moving. The former case is called a compound jet, while the latter case is referred to as a free jet.

Previous investigations, both analytical and experimental, have dealt with laminar and turbulent cases of heated and isothermal homogeneous free jets, heated and isothermal homogeneous compound jets, and heterogeneous free and compound jets. Most recently, the emphasis has been placed upon the more important case of turbulent flow. Measurements of average velocity and concentration in the similarity region of unbounded flow fields with determination of turbulent shear stresses and eddy viscosities have been made by a number of people. In most recent publications, turbulence measurements have been made in the jet mixing region. These include axial and radial turbulence intensities in a homogeneous compound jet and axial turbulence intensities in a heterogeneous compound jet.

The object of this work is to present turbulence data in both the early jet mixing region and further downstream for a ducted compound jet; that is, one in which the outer fluid stream cannot be considered infinite. The data includes average velocity profiles plus radial and axial turbulence intensity values for the homogeneous case. A heterogeneous ducted compound jet with Freon as the heavy inner fluid is also studied.

Data for this case consists of average velocity and average concentration profiles in addition to axial turbulence intensities.

The flow system consisted of a circular Freon 12 stream issuing into a coaxially flowing, ducted air stream. The flow is considered isothermal as well as subsonic and incompressible, since the velocities ranged from 1.5 ft/sec to 40 ft/sec. Turbulence quantities were measured by a constant temperature hot-film anemometer system. The air-Freon density ratio was 1/4, and the outer to inner velocity ratio ranged from 4.9 to 30.0.

BACKGROUND

There are four fundamental and presently acceptable concepts of turbulent transport which have been proposed; (1) Prandtl's old mixing length theory[1], (2) Prandtl's new mixing length theory[2], (3) Taylor's hypothesis[3], and (4) Reichardt's theory of turbulence[4].

Some investigators in the field of turbulent jets examined the turbulent mixing characteristics analytically by using one of the above mentioned transport theories. Kuethe[5] applied Prandtl's old mixing length theory to the problem of two parallel streams of the same composition moving at different velocities, while Tollmien[6] used the same theory to obtain a solution for the free circular jet problem. In 1942 Goertler[7] studied the free jet boundary and the two-dimensional free jet problem using Prandtl's new mixing length formulation. Squire and Trouncer[8] in 1943 applied this formulation to the case of a circular jet issuing into a general stream of the same composition and temperature. Using the constant exchange coefficient suggested by Prandtl, Torda and Stillwell[9] studied several jet mixing problems. In 1954, Torda, Thompson and Genetti[10] made an analysis of the initial mixing region for two-dimensional parallel jets and for coaxially flowing symmetric jets.

Other investigators attacked the problem of turbulent mixing by making experimental measurements of turbulent quantities in a number of systems using varied experimental techniques. A few were concerned with determining the eddy viscosity as a function of the flow field characteristics. These important experimental results served as a needed check on the analytical solutions which had been presented.

Liepmann and Laufer[11] experimentally studied the two-dimensional half-jet and compared their results with those of Tollmien and Goertler.

Forstall and Shapiro[12] worked with the mixing of coaxial jets and tested their results against the Squire and Trouncer analysis.

Very few experiments have been performed on the measurement of turbulent quantities in coaxial flows. Corrsin[13] as early as 1950 reported measurements of turbulence intensities in a homogeneous jet using a hot wire anemometer. Tani and Kobashi[14] used the same technique to make the first turbulence intensity measurements for the case of a homogeneous coaxial compound jet.

Experimental data for heterogeneous turbulent mixing is quite uncommon. Conger[15] made experimental measurements of heterogeneous turbulence behind a grid. Rosensweig[16] evaluated concentration fluctuations in a jet optically, while similar measurements have been made with an aspirator probe in a free jet by Blackshear and Fingerson[17].

Alpinieri[18] studied a heterogeneous jet and obtained values of local eddy viscosities. Boehman[19] developed expressions for eddy viscosity in a heterogeneous constant density coaxial flow field which gave the latter as a function of radial position across the jet orifice and of axial position downstream.

The most thorough turbulence measurements for heterogeneous coaxial jets have been done by Zawacki[20] and by D'Sousa[21]. Zawacki obtained values for turbulence intensities in both the near and far downstream regions using a hot wire anemometer for a number of velocity ratios and density ratios. Average velocity profiles and average density profiles were given along with radial turbulence intensities for the homogeneous case only.

D'Sousa presented axial turbulence intensities for a heterogeneous compound jet and showed a similarity between intensity profiles of a homogeneous jet and those of a heterogeneous jet.

Practically no work has been done with the topic of confined or "ducted" jets. A few experimental studies have been carried out by Hill[22], Curtet[23] and Curtet and Ricou[24].

Johnson and Clark[26] investigated a double compound cocurrent jet. They measured both the velocity and concentration of a heterogeneous system. Their pictures and graphs reenforce the arguments for recirculation patterns as presented by Zawacki.

ANALYTICAL METHODS

The basic instrument used in this investigation was the constant temperature hot-wire anemometer. The hot wire system is stable, accurate and has a short enough response time for turbulent flow measurements. The use of hot-film probes gives the added feature of durability and longivity.

Hot wire anemometry had its beginning with the study of heat transfer from small heated cylinders by King[25]. On the basis of potential flow around the wire he found that the heat loss was a linear function of the square root of velocity. This can be written as follows:

$$P = A + BU^{1/2} \tag{1}$$

Both A and B can be calculated in terms of geometry and physical properties. However, in practice, the coefficients A and B are determined by actual calibration.

Homogeneous System

A single wire probe may be used to find the axial turbulence intensity. By writing equation 1 as a linear combination of average and fluctuating components of velocity and power, squaring, time averaging, taking the square root and rearranging it becomes:

$$\frac{2\sqrt{\overline{p'^2}}}{\bar{P} - A} = \frac{\sqrt{\overline{u'^2}}}{\bar{U}} \tag{2}$$

The quantity $\frac{\sqrt{\overline{u'^2}}}{\bar{U}}$ is the axial turbulence intensity based on the average local velocity.

The axial as well as radial turbulence intensities may be found by means of an X-array probe. Writing the power lost by each of the two wires forming the X in terms of the geometry yields:

$$\frac{\sqrt{\overline{u'^2}}}{\bar{U}} = \frac{1}{2}\left[\left(\frac{\overline{4\,P'^2_1}}{(\bar{P}_1-A_1)^2} + \frac{\overline{4\,P'^2_2}}{(\bar{P}_2-A_2)^2} + 2\,\frac{\overline{(P'_1+P'_2)^2} - \overline{(P'_1-P'_2)^2}}{(\bar{P}_1-A_1)(\bar{P}_2-A_2)}\right)\right]^{1/2} \qquad (3)$$

$$\frac{\sqrt{\overline{v'^2}}}{\bar{U}} = \frac{1}{2}\left[\left(\frac{\overline{4P'^2_1}}{(\bar{P}_1-A_1)^2} + \frac{\overline{4\,P'^2_2}}{(\bar{P}_2-A_2)^2} - 2\,\frac{\overline{(P'_1+P'_2)^2} - \overline{(P'_1-P'_2)^2}}{(\bar{P}_1-A_1)(\bar{P}_2-A_2)}\right)\right]^{1/2} \qquad (4)$$

Hetrogeneous System

King[25] showed that both A and B in equation 1 are functions of the composition or density of the flow past the wire. Thus the power dissipated by the wire becomes a function of both velocity and composition.

A special hot-film sensor called an aspirating probe is used to determine the average density and a lower limit of the fluctuating density. Its construction will be discussed later.

Knowing the average density, the appropiate values for A and B for a single hot wire probe can be interpolated from a calibration curve. Thus the average velocity at a point where the average density is known and assumed to be constant for a given set of jet conditions, can be found from the power dissipated from a single hot wire probe.

Use of a pair of hot wire probes of differing geometry placed at the same point should allow determination of a set of unique values for $\overline{\rho'^2}$, $\overline{\rho'u'}$ and $\overline{u'^2}$. The values of $\overline{\rho'^2}$ taken by the aspirating probe are experimentally damped by mixing in the throat of a sonic nozzle. This, in addition to the fact that the values of $\overline{\rho'^2}$ are very small prevents exact solution of the three equations in three unknowns. Thus a method of finding $\overline{\rho'u'}$ and $\overline{u'^2}$ were needed. Montealegre[27] devised a method of incrementing $\overline{\rho'^2}$ to yield reasonable values of $\overline{\rho'u'}$ and $\overline{u'^2}$. This method was employed in finding the velocity turbulence intensities.

EXPERIMENTAL TECHNIQUE

Apparatus

Figure 1 shows the cocurrent coaxial ducted jet used in this study. The jet essentially consists of three sections; (1) a square reducing entrance section, (2) a three foot length of 6 inch I.D. sheet metal duct in which a 2.8 inch I.D. inner aluminum tube was mounted coaxially, and (3) a four foot length of 6 inch I.D. Lucite duct, the middle 2 1/2 feet of which served as the turbulent mixing test area. The lower one foot length of the plastic duct was stacked with cardboard honeycomb to prevent any exit effects such as swirling of the fluid.

The inner stream gas, air or Freon-12, was pressure fed in the top end of the tube after being metered through rotameters. A 1/8 inch thick fritted glass disk was mounted across the entrance to the aluminum tube to achieve full pipe flow. The outside of the lower open end of the tube was machine tapered from 0.082 inches to 0.005 incehs over an 18 inch length. This provided a smooth transition from annular to mixed flow. The Lucite duct was joined at both ends to the sheet metal duct by flanges and sealed by o-rings.

An air filter was placed across the top of the entrance section to prevent possible dust damage to the sensors. The sheet metal duct was made long enough to ensure parallel flow with a small boundary layer buildup, and to damp out large scale turbulence in the outer stream.

To eliminate turbulence and temperature effects of the blower, the outer air stream was sucked through the test section instead of being blown through. The bottom of the Lucite duct was connected to the suction end of the blower by 8 inch diameter sheet metal tubing. The output of the Buffalo, type 6E, low pressure drop, high capacity, 15 horsepower, centrifugal blower was controlled by an adjustable vane in the entrance line. A method for measuring the volumetric flow rate through the blower was not provided.

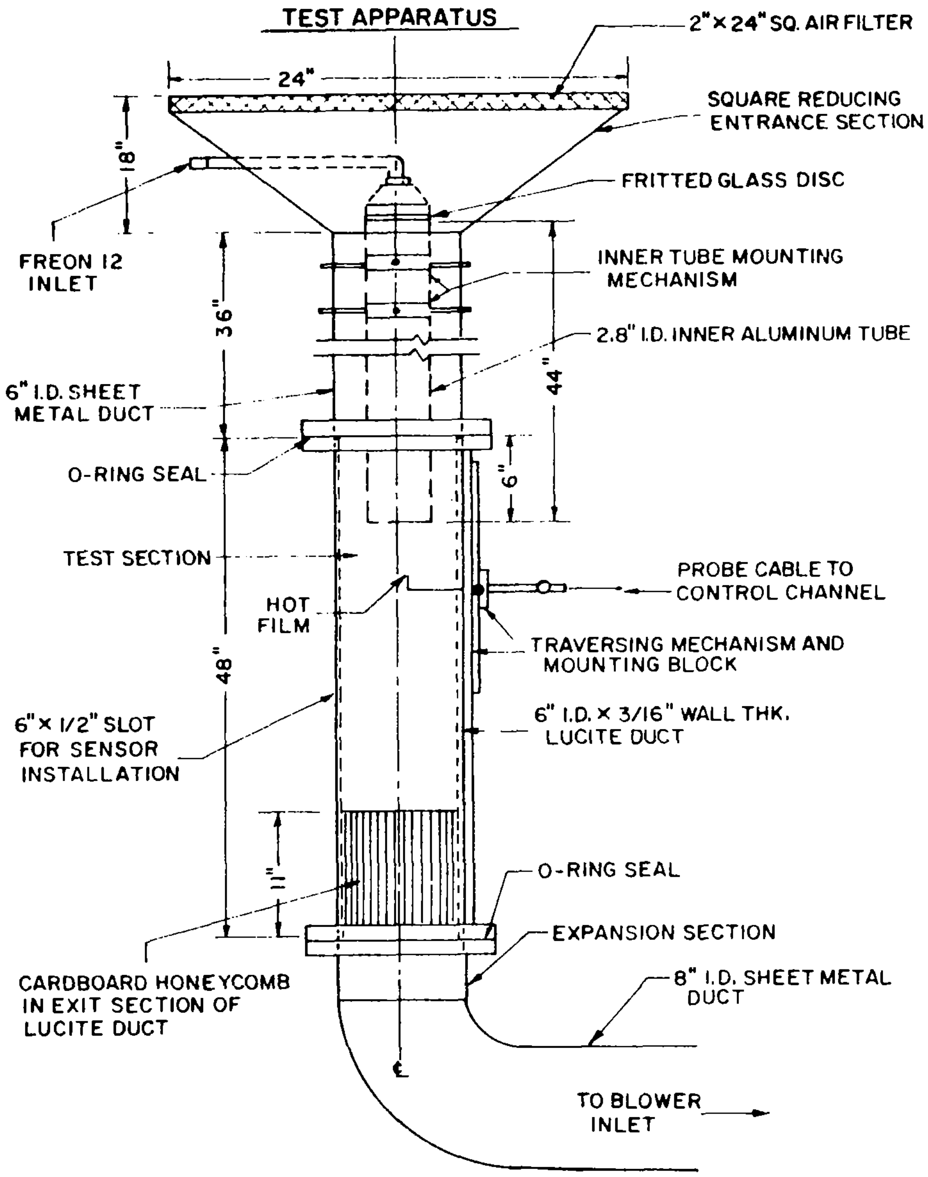
TEST APPARATUS
2"×24" SQ. AIR FILTER
24"
18"
SQUARE REDUCING ENTRANCE SECTION
FRITTED GLASS DISC
FREON 12 INLET
INNER TUBE MOUNTING MECHANISM
36"
2.8" I.D. INNER ALUMINUM TUBE
44"
6" I.D. SHEET METAL DUCT
O-RING SEAL
6"
TEST SECTION
PROBE CABLE TO CONTROL CHANNEL
HOT FILM
TRAVERSING MECHANISM AND MOUNTING BLOCK
48"
6" I.D. × 3/16" WALL THK. LUCITE DUCT
6"× 1/2" SLOT FOR SENSOR INSTALLATION
11"
O-RING SEAL
EXPANSION SECTION
CARDBOARD HONEYCOMB IN EXIT SECTION OF LUCITE DUCT
8" I.D. SHEET METAL DUCT
℄
TO BLOWER INLET

FIGURE 1

A 26 inch by 3/16 inch slot was milled through the wall of the test section and the traversing mechanism was mounted vertically on the Lucite duct. The traversing mechanism contained a gearing system which permitted radial and axial movement of the hot wire sensor along a plane containing the axis of the duct. Another small slot was milled through the wall of the Lucite duct to permit sensor installation.

Three high precision Brooks rotameters were used to meter the supply of Freon or air to the inner jet. The pressure was regulated upstream of the rotameters and was measured and the flow regulated downstream of the rotameters. Fine regulation of flow was achieved by use of small needle valves in parallel with the main globe valves. The rotameters were selected to allow a wide range of flow rates, from 0.06 SCFM to 50 SCFM of Freon-12 at 65 psig and from 0.1 SCFM to 90 SCFM of air at 40 psig within 1%.

The Freon-12 was supplied in 145 pound cylinders manifolded together. To compensate for the vaporization cooling, the cylinders were heated in a large jacketed steam vessel partially filled with water. The vessel could accomodate up to three tanks at a time, allowing a reasonable running capacity for the system. Since the Freon-12 was near its vapor pressure for the larger flow rates, a small electrical heating coil was used to further heat the Freon-12 supply line to raise its temperature and to prevent condensation in the rotameters.

The constant temperature hot wire system was purchased from Thermo Systems Inc. It consisted of two independent constant temperature channels, single, parallel , X-array and aspirator probes and related monitoring equipment. The monitoring equipment consisted of a digital voltmeter, an RMS meter, and a sum and difference unit.

Except for one of the two parallel wires, all sensors were of the hot film type. The four probes used were; a single wire probe, an aspirating probe, a parallel wire probe and a X-array probe. The wires were oriented in a plane perpendicular to the plane of the traversing mechanism and were connected to the probe holder by a ninety degree angle adapter. The sensors were thus allowed to be exactly oriented at the point of interest with no interference to the flow field. In the parallel wire probe, a 0.002 inch film and a 0.00015 inch wire were mounted 0.01 inch apart and parallel to each other on a single probe base.

The X-array probe was made up of two nearly identical films. The aspirator probe consisted of a 1 mil sensor mounted inside an 0.08 inch I.D. tube behind a jewel bearing with a hole of 0.008 inch. A vacuum pump sucked through the probe holder could sufficiently reduce the pressure downstream from the bearing to ensure sonic velocity at the throat of the bearing. Since the sonic velocity is strictly a function of composition of the gas, the power dissipated by the hot film is strictly a function of composition.

The calibration equipment consisted of a 15 foot section of 2 inch diameter schedule 40 pipe with its open end enclosed in a 6 inch by 6 inch by 36 inch plexiglass box which prevented stray room air currents from reaching the probe. The probe was held by a traversing mechanism mounted on the box. Freon and air rates were monitored by the three high precision Brooks rotameters. The gases were then passed through a mixing tee and then fed into the 2 inch pipe.

EXPERIMENTAL PROCEDURE

Homogeneous Case

Only the single hot-film and the X-array probe were needed for the homogeneous case. The average and RMS power input to the single hot-film sensor were needed to determine the average velocity and the axial turbulence intensity. To determine the radial turbulence intensity the average and RMS power input to each of the hot films on the X-array probe were taken along with the average sum and difference of the X-array probe.

Heterogeneous Case

The single hot film, the aspirator and the parallel probes were needed to determine the average velocity, average density and axial turbulence intensity.

The average power dissipation of the single hot film probe in cojunction with the average density given by the average power dissipated by the aspirator probe was used to find the average velocity. The RMS power dissipated by each of the parallel wires used in conjunction with the fluctuating density given by the RMS power dissipation of the aspirator probe was used to calculate the velocity turbulence intensity profiles.

CALCULATION PROCEDURE

Homeogeneous Case

The slope and intercept for each hot-film of the 2 probes used were found graphically. These were used in a simple computer program to determine average velocity, axial and radial turbulence intensities directly from the power dissipation of the probes.

Heterogeneous Case

For this case an average power versus density plot for the aspirator probe was needed in addition to a slope and intercept versus density plot for each of the hot wires on the single and parallel probes. The average density at a point was read off the average power versus density curve. The average density, the average power dissipation of the single wire probe and the RMS power dissipation of the aspirator and each of the parallel wires were used as inputs into the 360-40 computer to calculate the average velocity and axial turbulence intensities.

RESULTS AND DISCUSSION

Homogeneous Case

Figures 2 through 13 give the results of all homogeneous runs for velocity ratios of 5.8, 10.0, 14.7 and 30.0. In each case dimensionless velocity profiles are given along with axial and radial turbulence intensity profiles. The velocity profiles illustrate the existence of a momentum trough caused by the boundary layer buildup on both the inside and outside of the dividing tube wall. While the flow in the trough is being accelerated, the velocity at the centerline decreases. Once this trough disappears, the velocity profile is shown to be an increasing continuous curve with the minimum at the centerline while the maximum velocity is reached somewhere in the outer stream. The velocity then decreases to zero at the outer tube inner wall boundary. At each succeeding axial position downstream the central portion of the profile is accelerated and the outer region tends to flatten out. The axial position at which the centerline velocity stops decreasing and begins to increase depends upon the velocity ratio; the smaller the ratio, the farther downstream this point occurs, since a higher inner stream flow has greater momentum and hence tends to be preserved longer. *For instance, in figure 2 at a velocity ratio of 5.8 the centerline velocity* decreases from the mouth of the tube to an axial position greater than $z/r_o = 2.14$, but less than $z/r_o = 3.57$. At axial distances further downstream, the centerline velocity is shown to increase. At a velocity ratio of 10.0, as in figure 5, this transition point occurs closer to the tube exit, that is, between $z/r_o = 0.71$ and $z/r_o = 1.43$. Due to the presence of large fluctuations near the tube exit, the centerline velocity at still farther downstream positions decreased once more before finally increasing again. This behavior was also found by Zawacki.[20]

Zawacki also reported the occurance of large velocity fluctuations at the outlet of the tube which were not present without outer stream flow, indicating circulation patterns to be present.

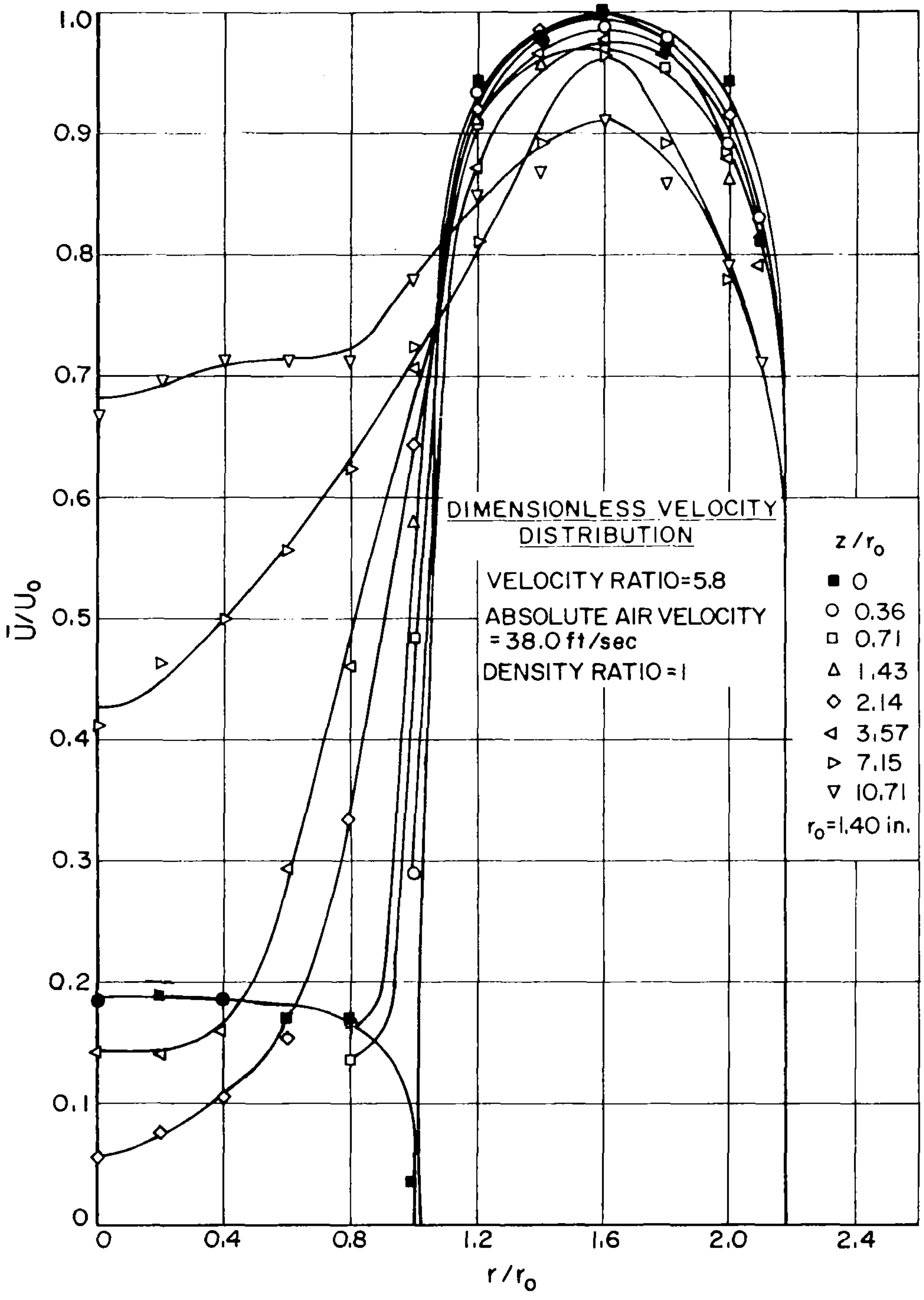
1.0
0.9
0.8
0.7
0.6
0.5
0.4
0.3
0.2
0.1
0
$\bar{U}/U_0$
0
0.4
0.8
1.2
1.6
2.0
2.4
r/r_0
DIMENSIONLESS VELOCITY DISTRIBUTION
VELOCITY RATIO=5.8
ABSOLUTE AIR VELOCITY =38.0 ft/sec
DENSITY RATIO=1
z/r_0
■ 0
○ 0.36
□ 0.71
△ 1.43
◇ 2.14
◁ 3.57
▷ 7.15
▽ 10.71
r_0=1.40 in.

FIGURE 2

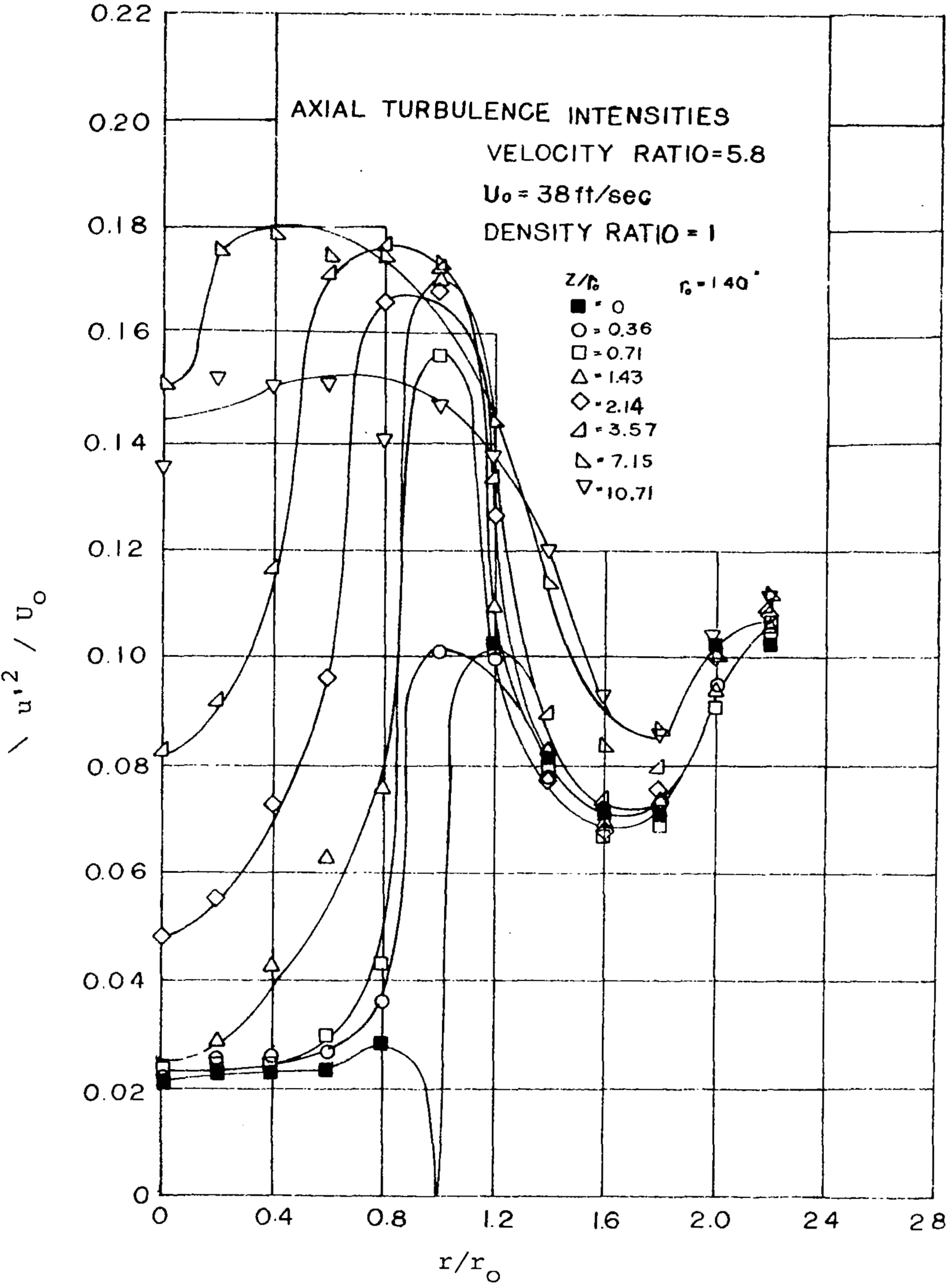
AXIAL TURBULENCE INTENSITIES
VELOCITY RATIO=5.8
U₀ = 38 ft/sec
DENSITY RATIO = 1
Z/r₀
r₀ = 1.40"
■ = 0
○ = 0.36
□ = 0.71
△ = 1.43
◇ = 2.14
◿ = 3.57
◺ = 7.15
▽ = 10.71
$\sqrt{\overline{u'^2}} / U_o$
0.22
0.20
0.18
0.16
0.14
0.12
0.10
0.08
0.06
0.04
0.02
0
0
0.4
0.8
1.2
1.6
2.0
2.4
2.8
r/r_o

FIGURE 3

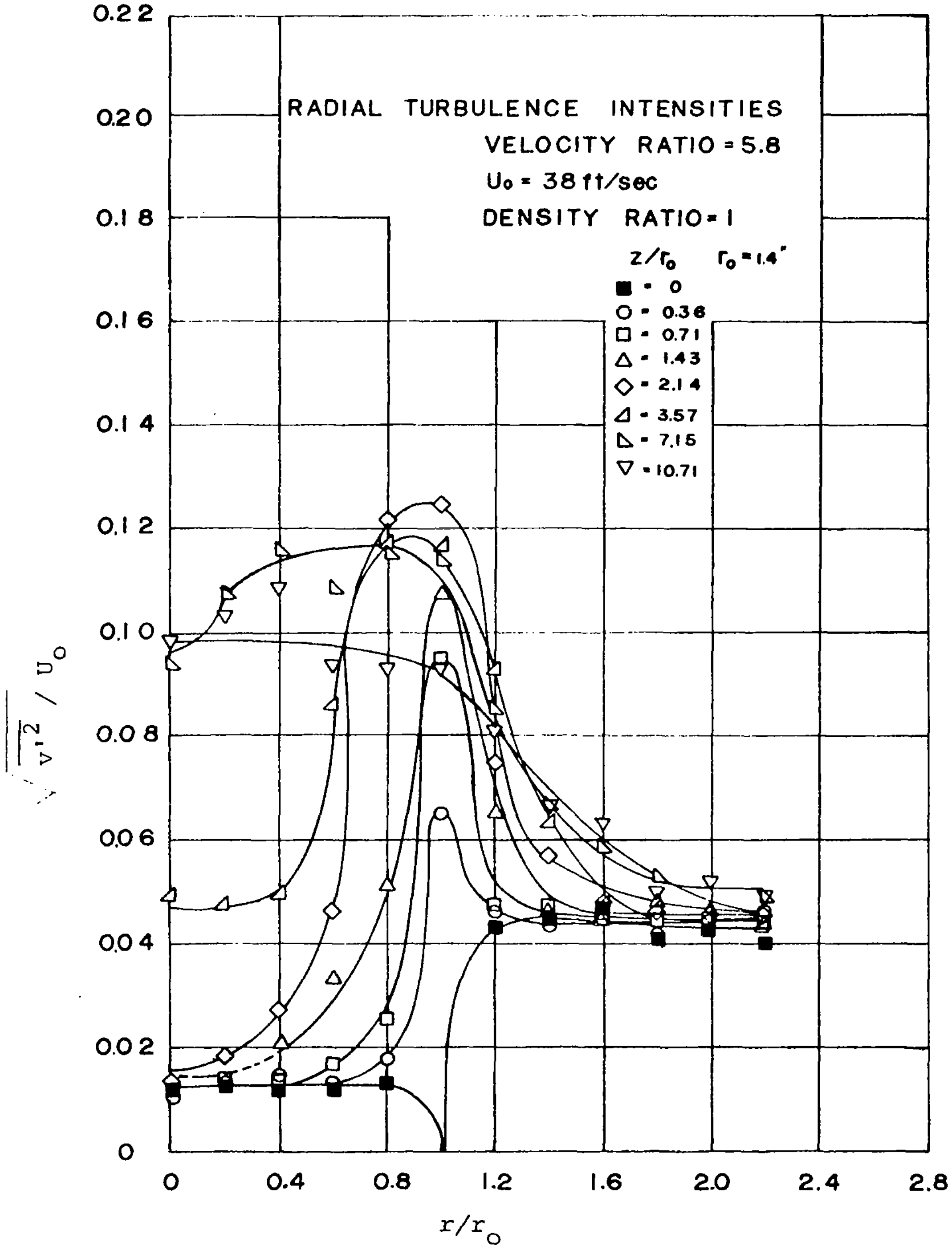
RADIAL TURBULENCE INTENSITIES
VELOCITY RATIO = 5.8
U₀ = 38 ft/sec
DENSITY RATIO = 1
z/r₀ r₀ = 1.4"
■ = 0
○ = 0.36
□ = 0.71
△ = 1.43
◇ = 2.14
◺ = 3.57
◹ = 7.15
▽ = 10.71
0.22
0.20
0.18
0.16
0.14
0.12
0.10
0.08
0.06
0.04
0.02
0
0.4
0.8
1.2
1.6
2.0
2.4
2.8
√v'² / U₀
r/r₀

FIGURE 4

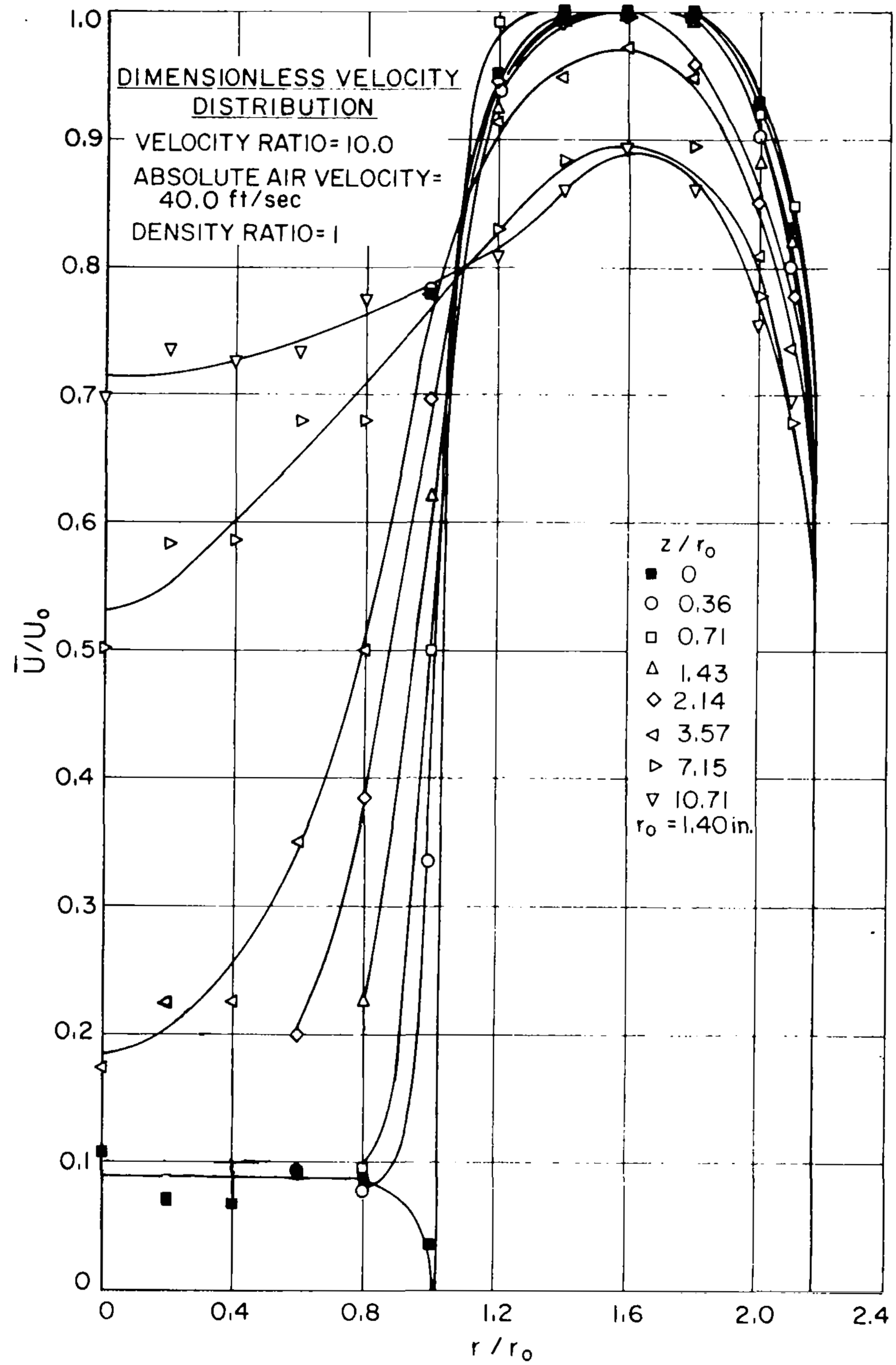
DIMENSIONLESS VELOCITY DISTRIBUTION
VELOCITY RATIO= 10.0
ABSOLUTE AIR VELOCITY= 40.0 ft/sec
DENSITY RATIO= 1
z / r_0
■ 0
○ 0.36
□ 0.71
△ 1.43
◇ 2.14
◁ 3.57
▷ 7.15
▽ 10.71
r_0 = 1.40 in.
$\bar{U}/U_0$
r / r_0
0
0.1
0.2
0.3
0.4
0.5
0.6
0.7
0.8
0.9
1.0
0
0.4
0.8
1.2
1.6
2.0
2.4

FIGURE 5

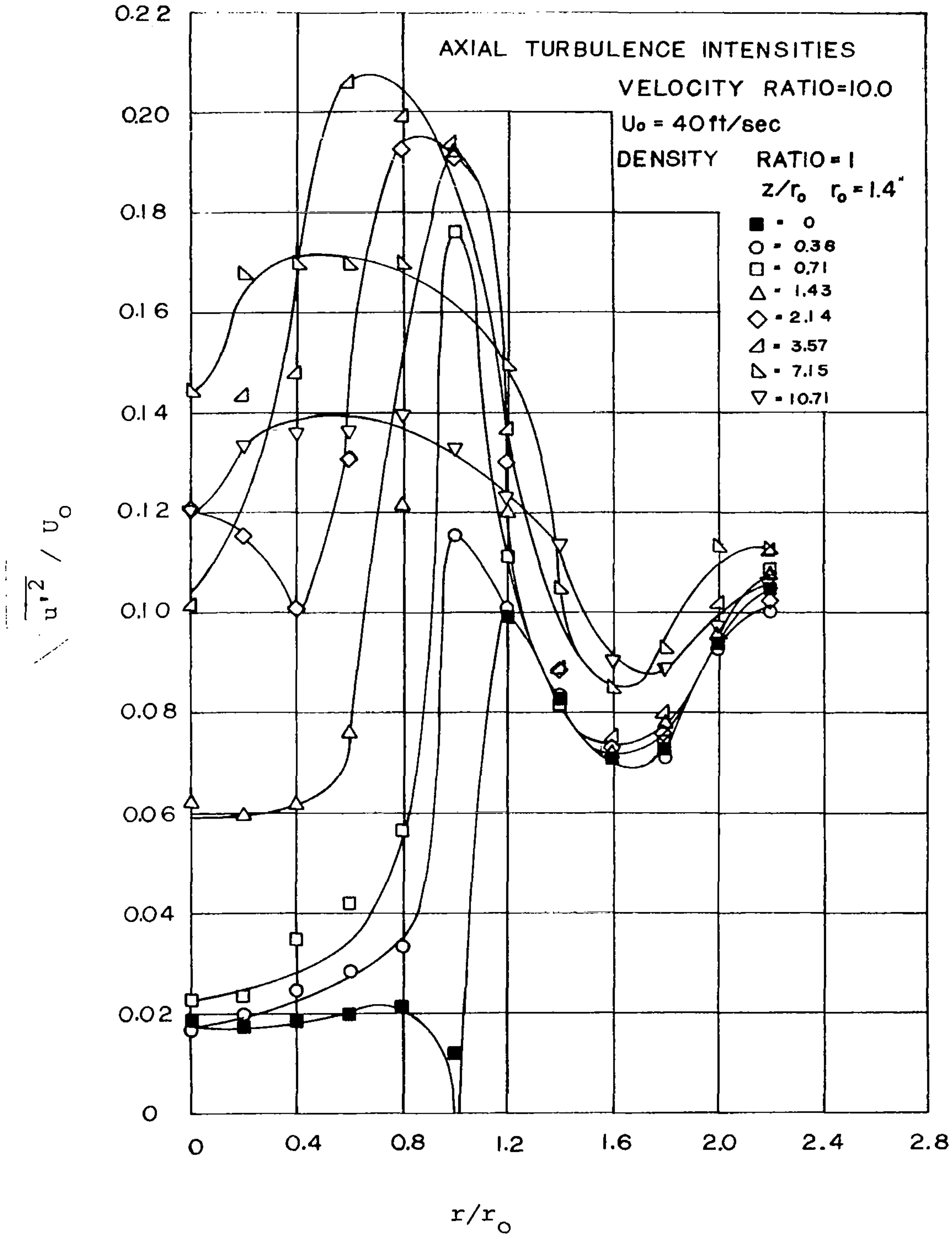
AXIAL TURBULENCE INTENSITIES
VELOCITY RATIO=10.0
Uo = 40 ft/sec
DENSITY RATIO = 1
Z/r₀ r₀ = 1.4"
■ = 0
○ = 0.36
□ = 0.71
△ = 1.43
◇ = 2.14
◿ = 3.57
◺ = 7.15
▽ = 10.71
0.22
0.20
0.18
0.16
0.14
0.12
0.10
0.08
0.06
0.04
0.02
0
0
0.4
0.8
1.2
1.6
2.0
2.4
2.8
$\sqrt{\overline{u'^2}} / U_o$
r/r_o

FIGURE 6

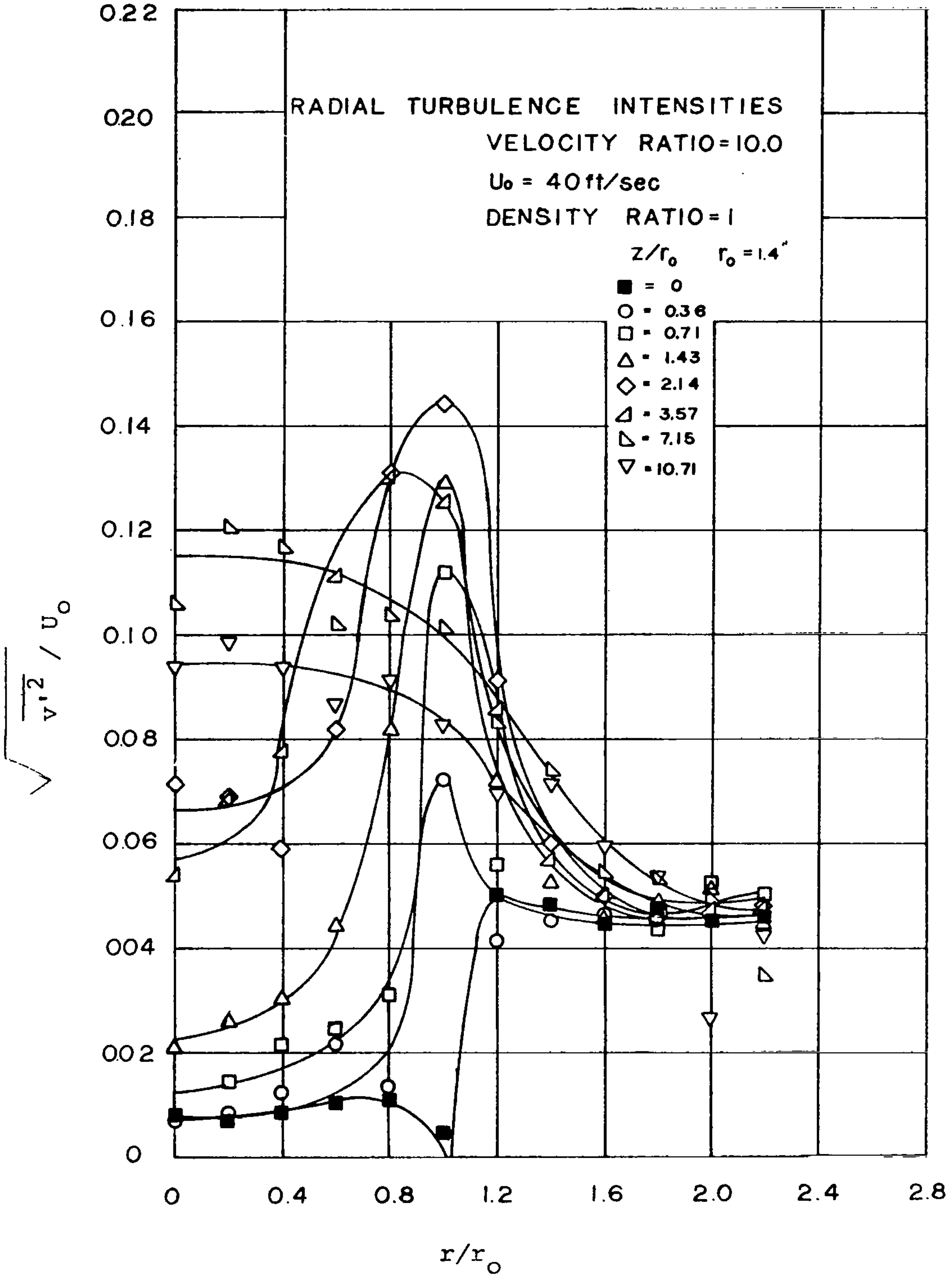
RADIAL TURBULENCE INTENSITIES
VELOCITY RATIO=10.0
U₀ = 40 ft/sec
DENSITY RATIO=1
Z/r₀ r₀ = 1.4"
■ = 0
○ = 0.36
□ = 0.71
△ = 1.43
◇ = 2.14
◿ = 3.57
◺ = 7.15
▽ = 10.71
0.22
0.20
0.18
0.16
0.14
0.12
0.10
0.08
0.06
0.04
0.02
0
$\sqrt{\overline{v'^2}} / U_0$
0
0.4
0.8
1.2
1.6
2.0
2.4
2.8
r/r₀

FIGURE 7

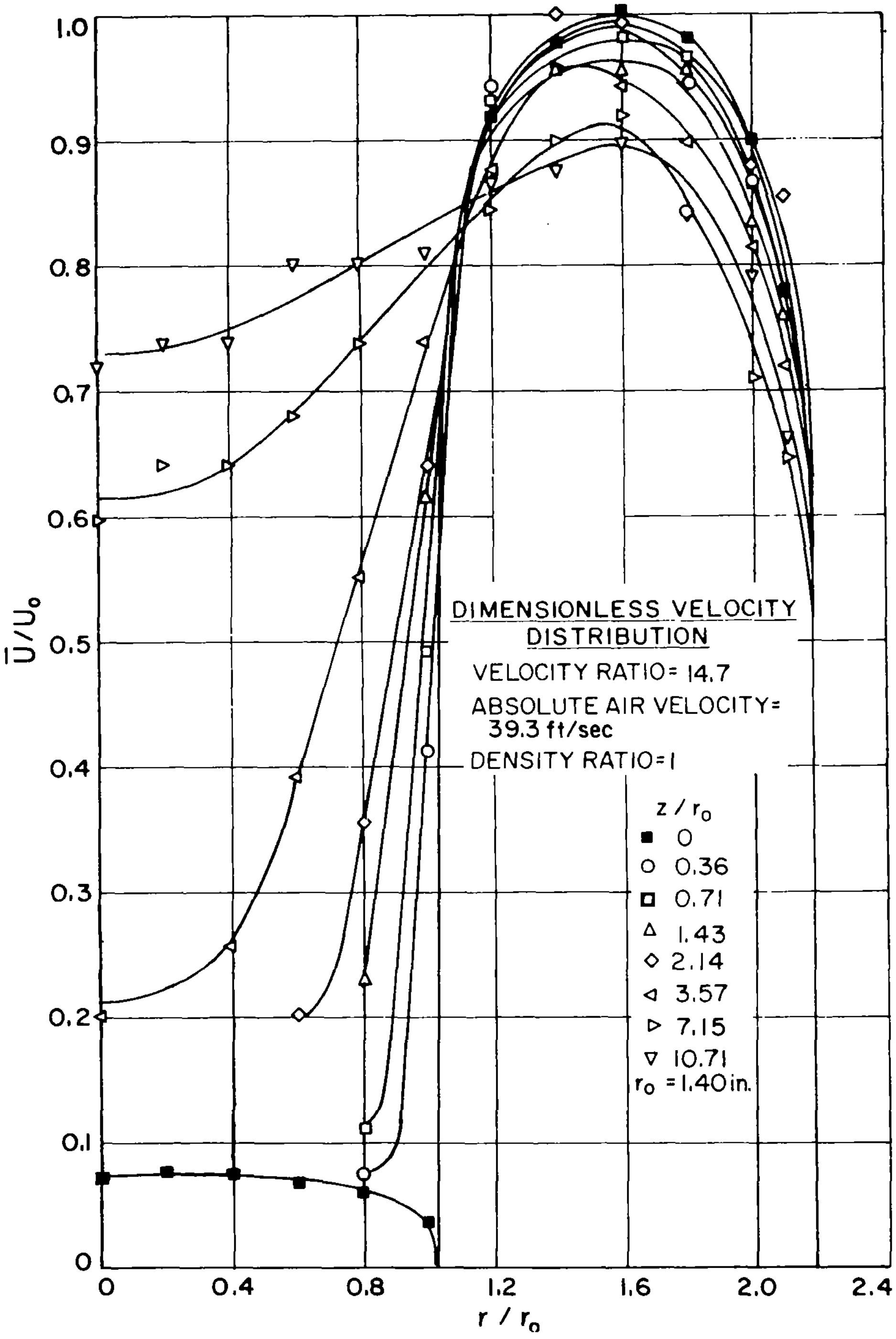

1.0
0.9
0.8
0.7
0.6
0.5
0.4
0.3
0.2
0.1
0
$\bar{U}/U_o$
0
0.4
0.8
1.2
1.6
2.0
2.4
r / r_o
DIMENSIONLESS VELOCITY DISTRIBUTION
VELOCITY RATIO= 14.7
ABSOLUTE AIR VELOCITY= 39.3 ft/sec
DENSITY RATIO=1
z / r_o
■ 0
○ 0.36
□ 0.71
△ 1.43
◇ 2.14
◁ 3.57
▷ 7.15
▽ 10.71
r_o =1.40 in.

FIGURE 8

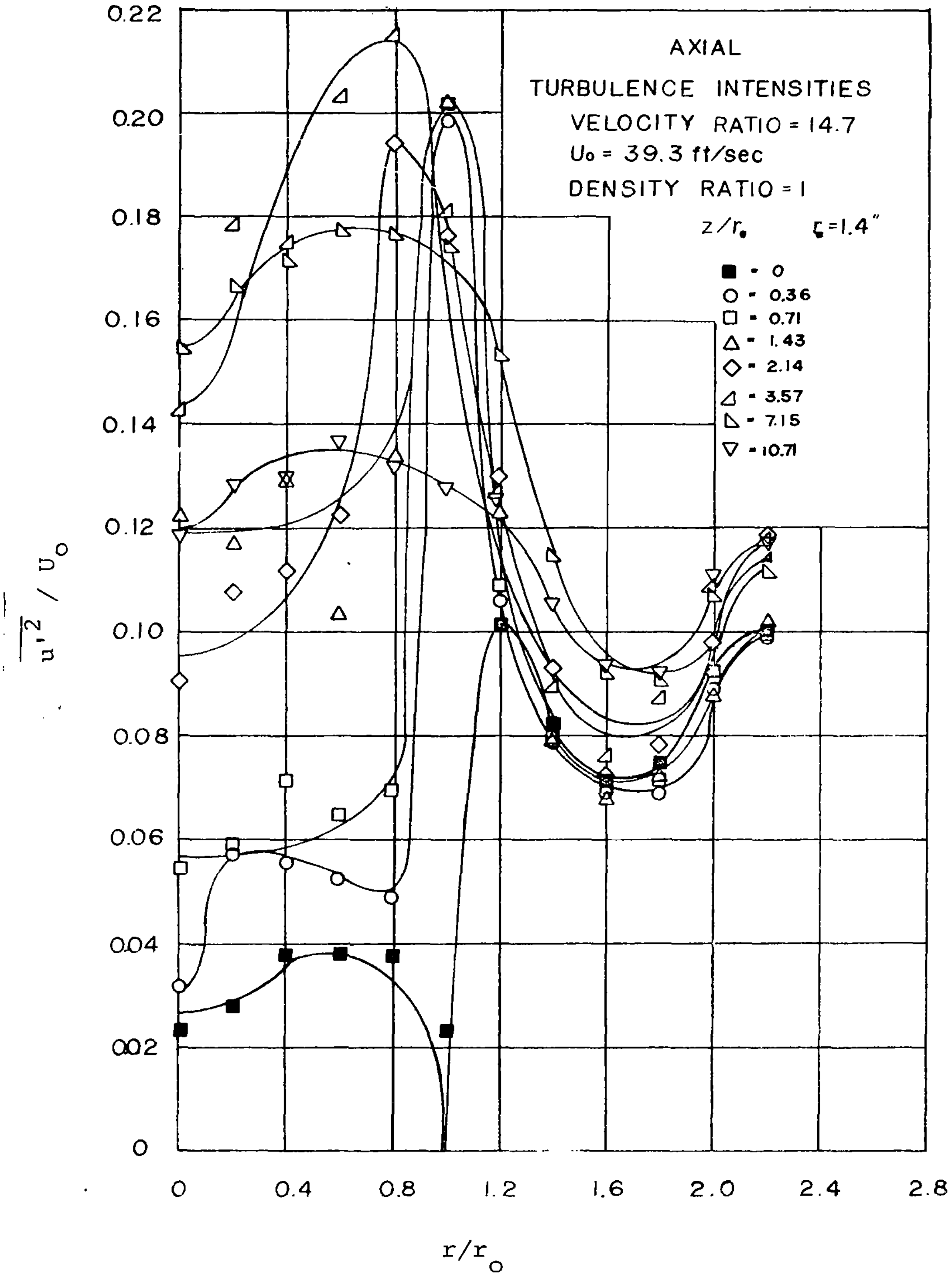
AXIAL
TURBULENCE INTENSITIES
VELOCITY RATIO = 14.7
Uo = 39.3 ft/sec
DENSITY RATIO = 1
z/r₀ r₀=1.4"
■ = 0
○ = 0.36
□ = 0.71
△ = 1.43
◇ = 2.14
◺ = 3.57
◣ = 7.15
▽ = 10.71
0.22
0.20
0.18
0.16
0.14
0.12
0.10
0.08
0.06
0.04
0.02
0
0
0.4
0.8
1.2
1.6
2.0
2.4
2.8
√(u'²) / U₀
r/r₀

FIGURE 9

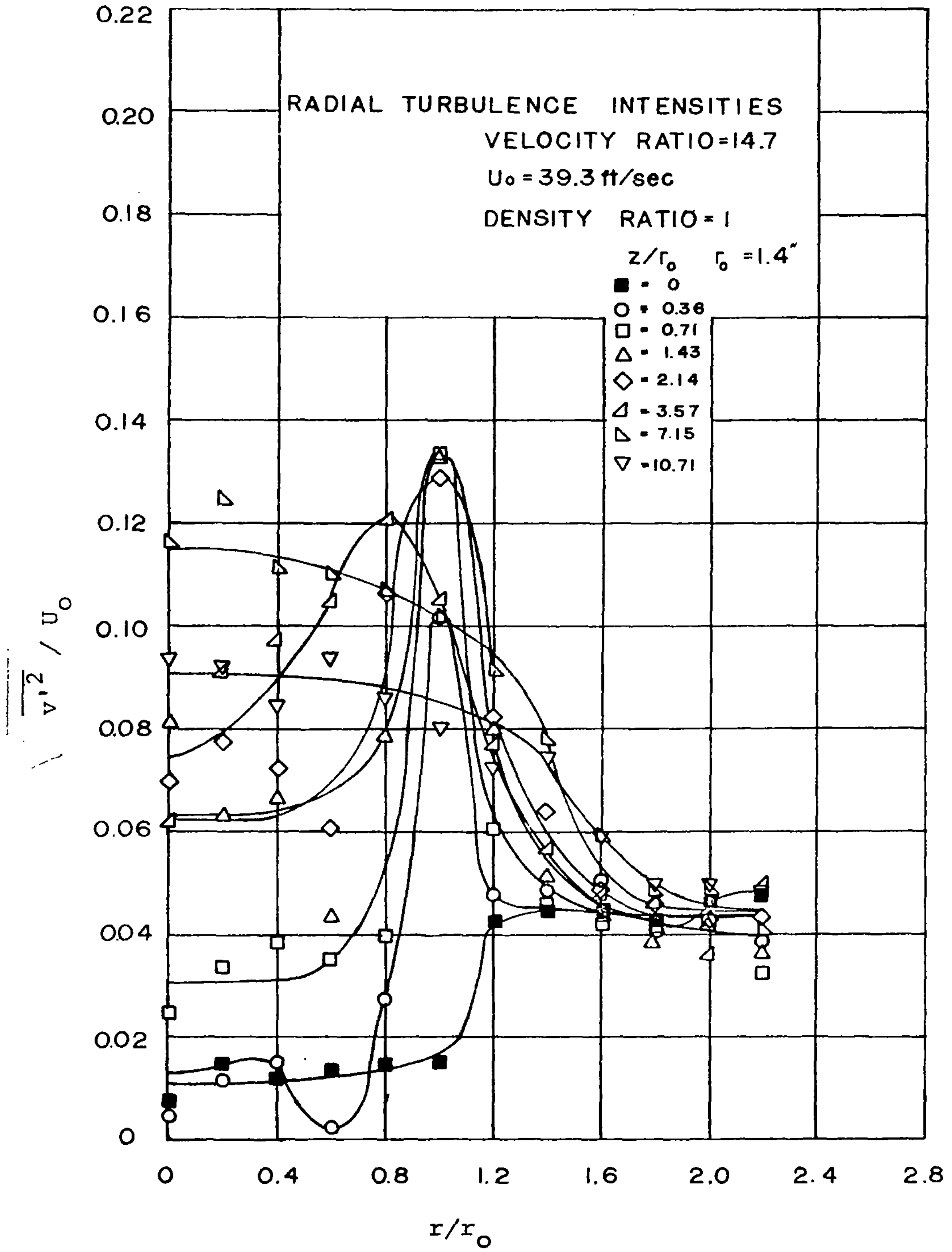
RADIAL TURBULENCE INTENSITIES
VELOCITY RATIO=14.7
Uo=39.3 ft/sec
DENSITY RATIO=1
z/r₀ r₀ =1.4"
■ = 0
○ = 0.36
□ = 0.71
△ = 1.43
◇ = 2.14
◺ = 3.57
◺ = 7.15
▽ = 10.71
0.22
0.20
0.18
0.16
0.14
0.12
0.10
0.08
0.06
0.04
0.02
0
0.4
0.8
1.2
1.6
2.0
2.4
2.8
√v'² / U₀
r/r₀

FIGURE 10

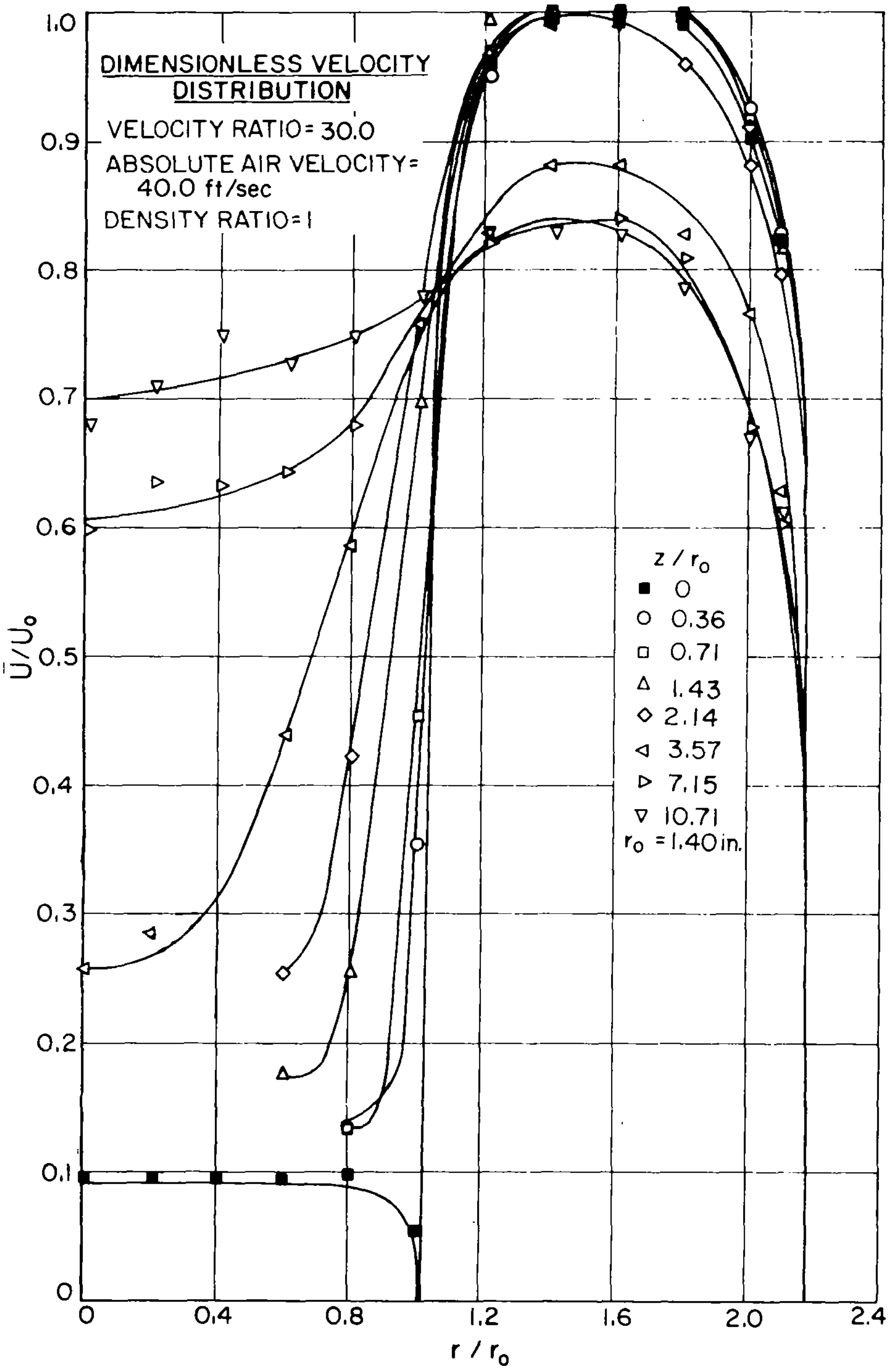
DIMENSIONLESS VELOCITY DISTRIBUTION
VELOCITY RATIO= 30.0
ABSOLUTE AIR VELOCITY= 40.0 ft/sec
DENSITY RATIO= 1
z / r_0
■ 0
○ 0.36
□ 0.71
△ 1.43
◇ 2.14
◁ 3.57
▷ 7.15
▽ 10.71
r_0 = 1.40 in.
$\bar{U}/U_0$
0
0.1
0.2
0.3
0.4
0.5
0.6
0.7
0.8
0.9
1.0
0
0.4
0.8
1.2
1.6
2.0
2.4
r / r_0

FIGURE 11

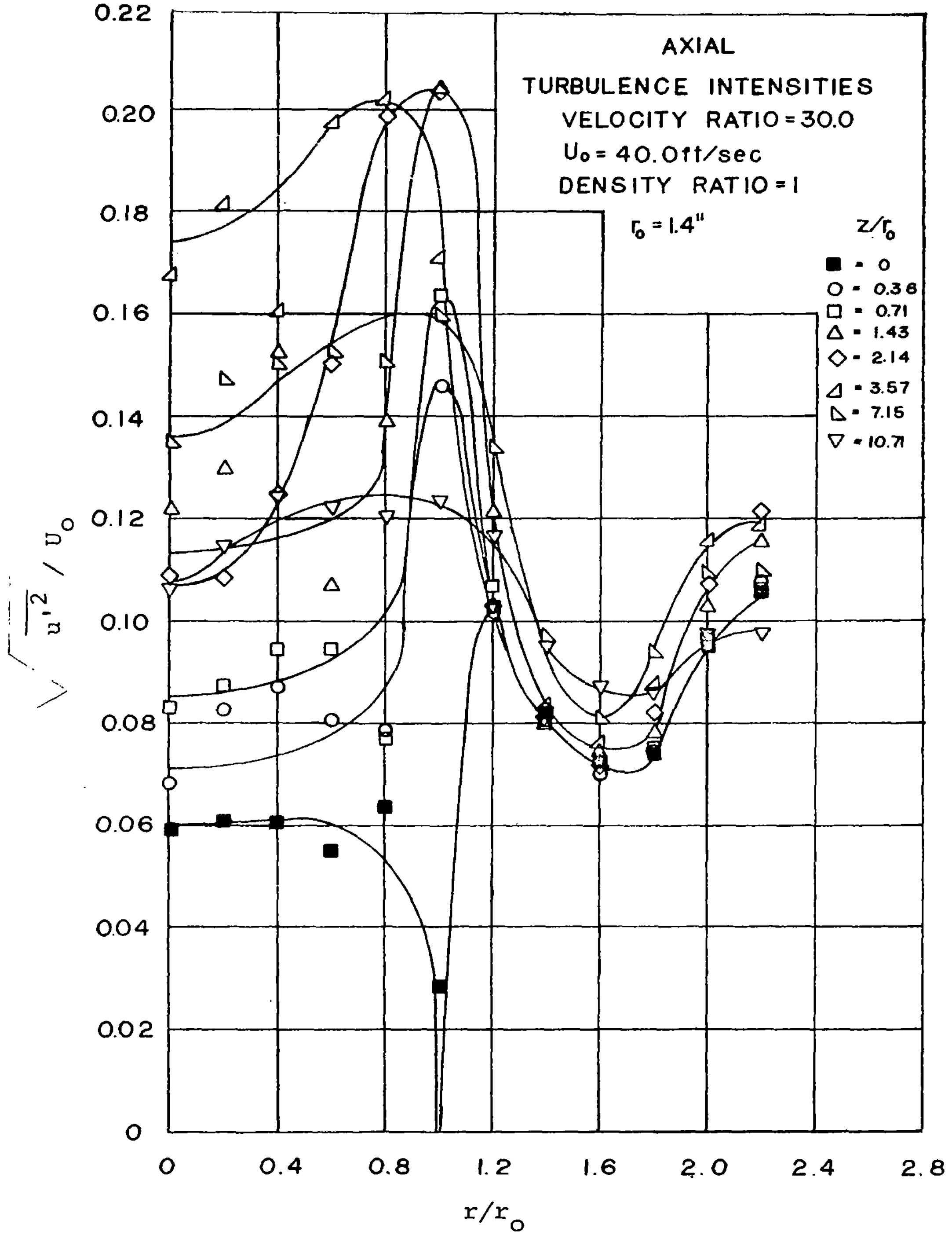
AXIAL
TURBULENCE INTENSITIES
VELOCITY RATIO = 30.0
U_o = 40.0 ft/sec
DENSITY RATIO = 1
r_o = 1.4"
z/r_o
■ = 0
○ = 0.36
□ = 0.71
△ = 1.43
◇ = 2.14
◺ = 3.57
◹ = 7.15
▽ = 10.71
0.22
0.20
0.18
0.16
0.14
0.12
0.10
0.08
0.06
0.04
0.02
0
$\sqrt{\overline{u'^2}} / U_o$
0
0.4
0.8
1.2
1.6
2.0
2.4
2.8
r/r_o

FIGURE 12

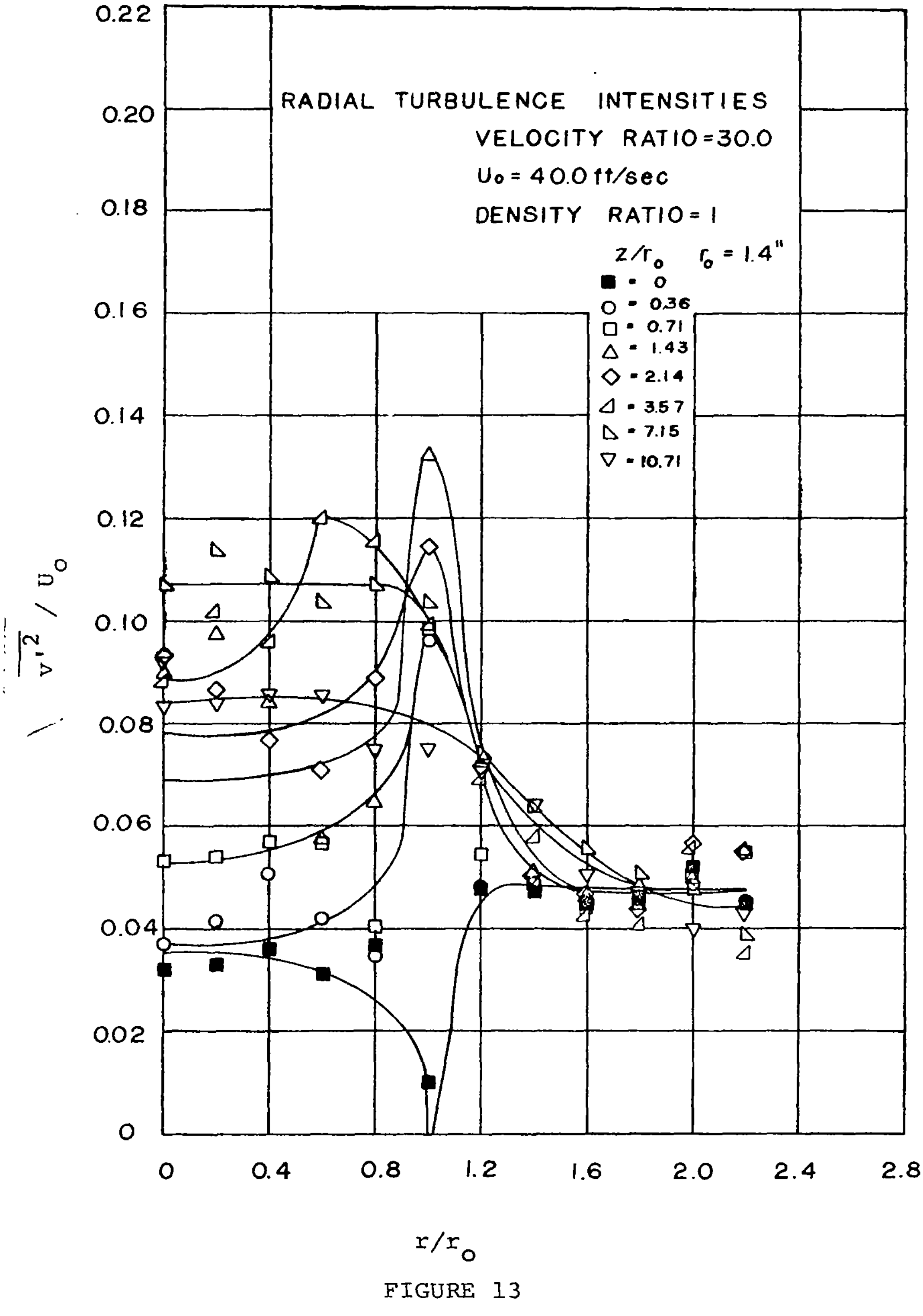
RADIAL TURBULENCE INTENSITIES
VELOCITY RATIO=30.0
U₀ = 40.0 ft/sec
DENSITY RATIO = 1
z/r₀ r₀ = 1.4"
■ = 0
○ = 0.36
□ = 0.71
△ = 1.43
◇ = 2.14
⊿ = 3.57
◺ = 7.15
▽ = 10.71
0.22
0.20
0.18
0.16
0.14
0.12
0.10
0.08
0.06
0.04
0.02
0
0
0.4
0.8
1.2
1.6
2.0
2.4
2.8
√(v'²) / U₀
r/r₀

FIGURE 13

This effect is due to the sudden expansion of the outer stream around the end of the inner tube. The fluid is thought to move in radially and converge at the centerline. With small inner stream flows the fluid then moves into the tube setting up the circulation patterns. Since information such as whether velocity components are either positive or negative is not attainable using a hot wire anemometer, the circulation patterns can only be estimated. No measurements for velocity are reported where it was felt backflow was present.

The axial and radial turbulence intensity profiles were found to be remarkably similar both in shape and magnitude. For most velocity ratios, the turbulence intensity was found to increase with downstream position and reach a maximum between a z/r_o of 2 and 5. It then decreased for $z/r_o > 5$. The turbulent intensity profiles show that a peak value was reached, usually for $1.0 \leq r/r_o \leq 0.8$. Moving into the outer stream region, the axial turbulence intensities decrease to about 6% to 9% then increased to about 10%to 12% near the wall (approximately 0.1 inch away). The ratio of axial turbulence to radial turbulence (u'/v') was usually about 1.5 as was noted by Zawacki for unbounded coaxial flow. Thus, each turbulence intensity profile is characterized by a maximum turbulence intensity which is larger than the centerline turbulence intensity by an amount which depends upon the axial distance downstream.

Heterogeneous Case

The heterogeneous dimensionless velocity profiles are shown in figures 14, 17, 20 and 23 for four velocity ratios. Essentially, they illustrate the same flow characteristics as did the homogeneous velocity profiles and reiterate the momentum trough hypothesis. However, the heterogeneous profiles show that due to the higher density of the Freon, momentum transfer is considerably less than in the homogeneous case. This result is most clearly illustrated at low velocity ratios. Comparing figure 2 with figure 14 at the $z/r_o = 10.71$ position, it is seen that the heterogeneous velocity at the centerline is approximately one half the homogeneous centerline velocity for about the same velocity ratio.

The density profiles, shown in figures 15, 18, 21 and 24, also behave as would be expected. For a distance downstream of the tube exit, there is a cone-shaped region of pure Freon-12 which is usually termed the potential core region of concentration. As one proceeds from one axial position to another, the outermost point of the pure Freon region moves inward toward the centerline. After the end of the potential core region is reached, a sharp decline occurs in the concentration. As the velocity ratio is decreased, the point at which the potential core for concentration ends moves farther downstream. For example, in figure 15 the potential core region ends after a z/r_o position of 1.43 as compared to figure 24 where the potential core ends somewhere between the tube exit and $z/r_o = 0.36$.

The large fluctuations which were present in the homogeneous case, occured in the heterogeneous case, but to a somewhat lesser extent. It is assumed that this is due to a backflow region which also covers the humps in two of the density profiles in figure 24.

Heterogeneous axial turbulence intensities are shown in figures 16, 19, 22 and 25. The shapes of the turbulence intensity profiles are similar to those of the homogeneous case, are somewhat smaller in magnitude. The maximum heterogeneous turbulence intensity obtained was slightly greater than that of the homogeneous case.

Figure 26 is a plot of the mass holdup as a function of downstream position. The first profile taken at a velocity ratio of 4.9 shows the potential core and mixed flow phenomena. The next two profiles taken at velocity ratios of 9.5 and 13.8 respectively show little difference. This region of velocity ratios could be termed the transition region where both the wake-potential core flow and backflow occur

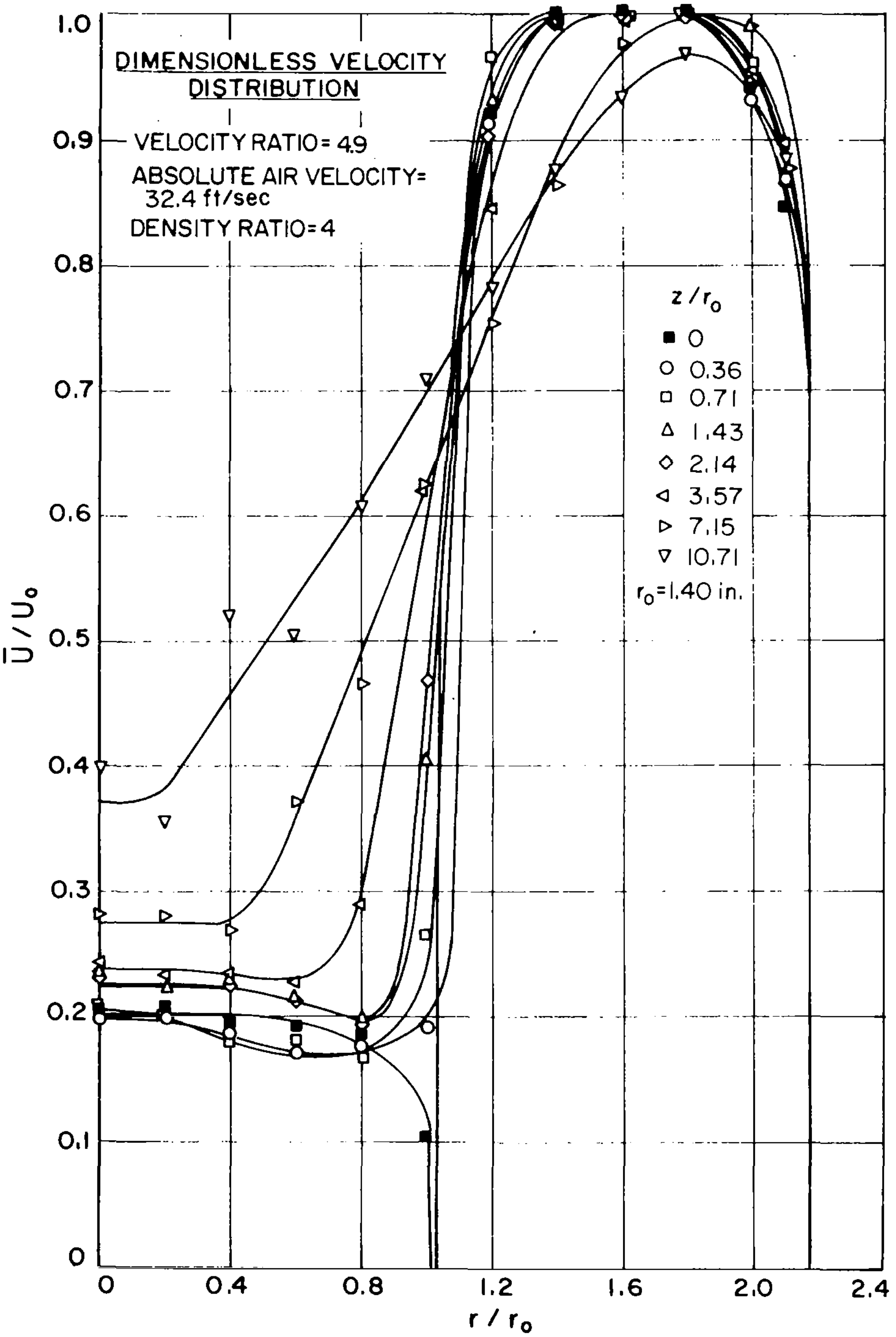
DIMENSIONLESS VELOCITY DISTRIBUTION
VELOCITY RATIO= 4.9
ABSOLUTE AIR VELOCITY= 32.4 ft/sec
DENSITY RATIO= 4
z/r_o
■ 0
○ 0.36
□ 0.71
△ 1.43
◇ 2.14
◁ 3.57
▷ 7.15
▽ 10.71
r_o=1.40 in.
$\bar{U}/U_o$
1.0
0.9
0.8
0.7
0.6
0.5
0.4
0.3
0.2
0.1
0
0
0.4
0.8
1.2
1.6
2.0
2.4
r/r_o

FIGURE 14

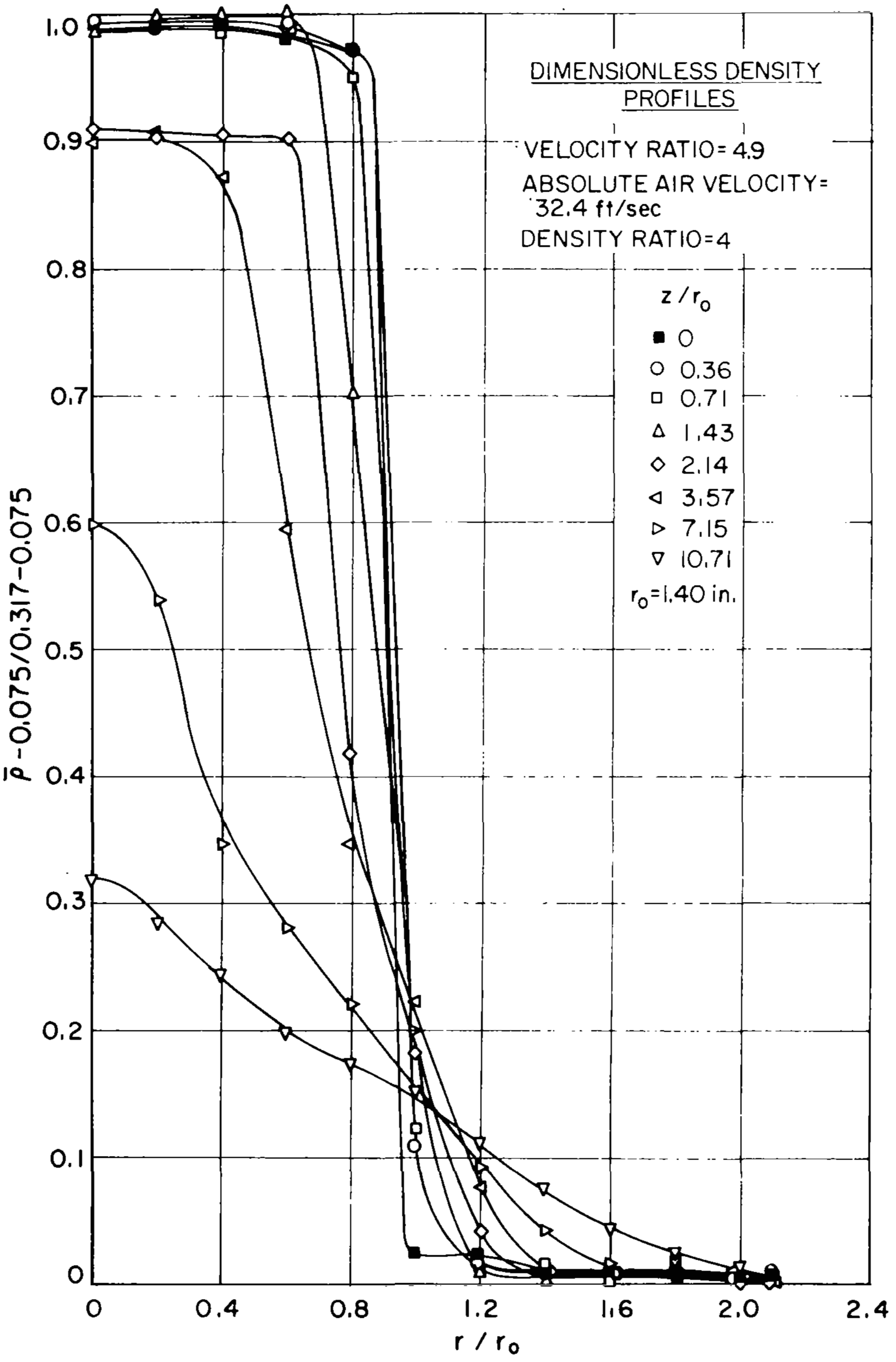

DIMENSIONLESS DENSITY PROFILES
VELOCITY RATIO= 4.9
ABSOLUTE AIR VELOCITY= 32.4 ft/sec
DENSITY RATIO=4
z/r_0
■ 0
○ 0.36
□ 0.71
△ 1.43
◇ 2.14
◁ 3.57
▷ 7.15
▽ 10.71
r_0=1.40 in.
$\bar{\rho}$-0.075/0.317-0.075
1.0
0.9
0.8
0.7
0.6
0.5
0.4
0.3
0.2
0.1
0
0
0.4
0.8
1.2
1.6
2.0
2.4
r/r_0

FIGURE 15

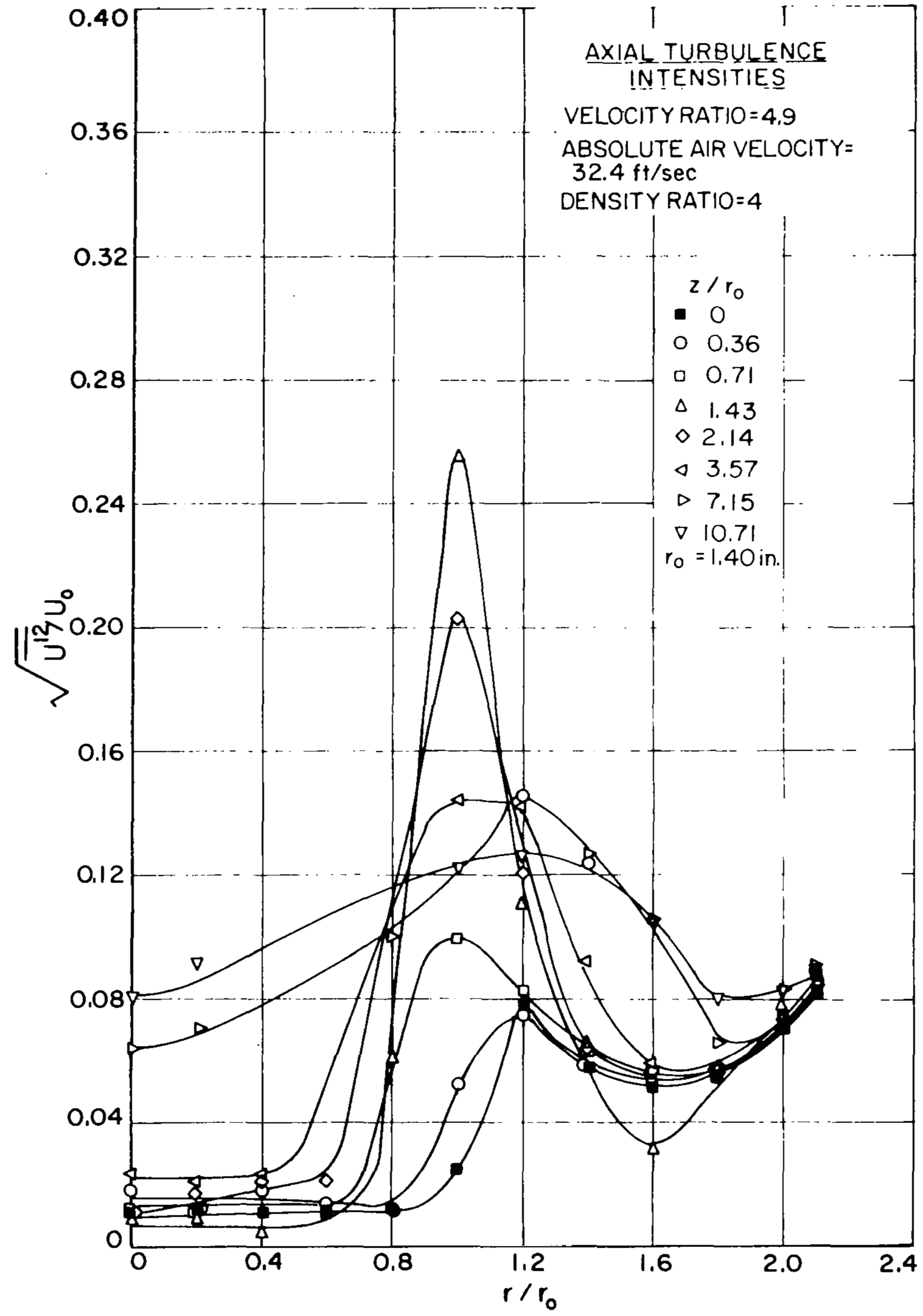
AXIAL TURBULENCE INTENSITIES
VELOCITY RATIO=4.9
ABSOLUTE AIR VELOCITY= 32.4 ft/sec
DENSITY RATIO=4
z / r_o
■ 0
○ 0.36
□ 0.71
△ 1.43
◇ 2.14
◁ 3.57
▷ 7.15
▽ 10.71
r_o = 1.40 in.
$\sqrt{\overline{u'^2}}/U_o$
0
0.04
0.08
0.12
0.16
0.20
0.24
0.28
0.32
0.36
0.40
0
0.4
0.8
1.2
1.6
2.0
2.4
r / r_o

FIGURE 16

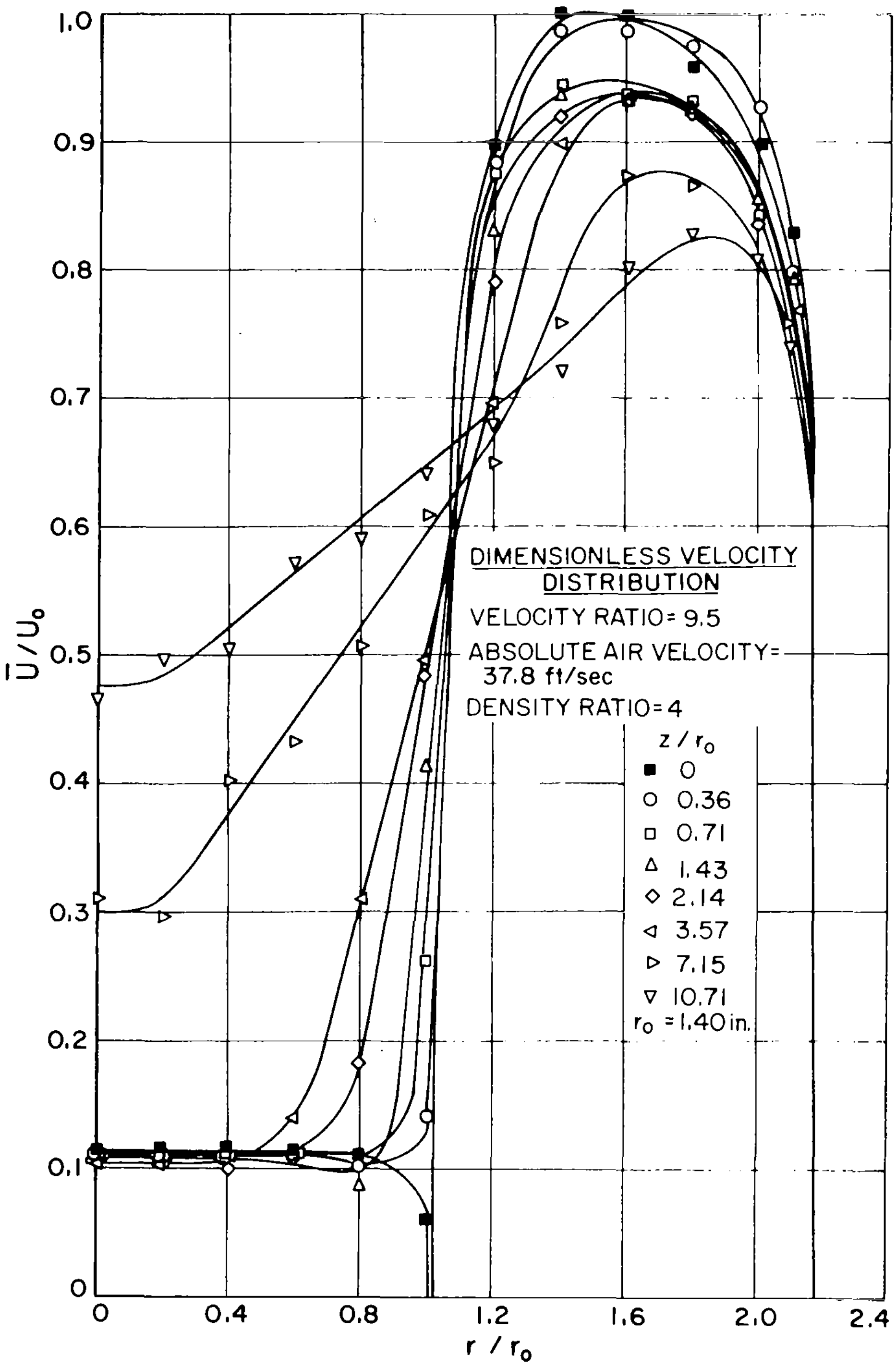
DIMENSIONLESS VELOCITY DISTRIBUTION
VELOCITY RATIO= 9.5
ABSOLUTE AIR VELOCITY= 37.8 ft/sec
DENSITY RATIO= 4
z / r₀
■ 0
○ 0.36
□ 0.71
△ 1.43
◇ 2.14
◁ 3.57
▷ 7.15
▽ 10.71
r₀ = 1.40 in.
Ū / U₀
0
0.1
0.2
0.3
0.4
0.5
0.6
0.7
0.8
0.9
1.0
0
0.4
0.8
1.2
1.6
2.0
2.4
r / r₀

FIGURE 17

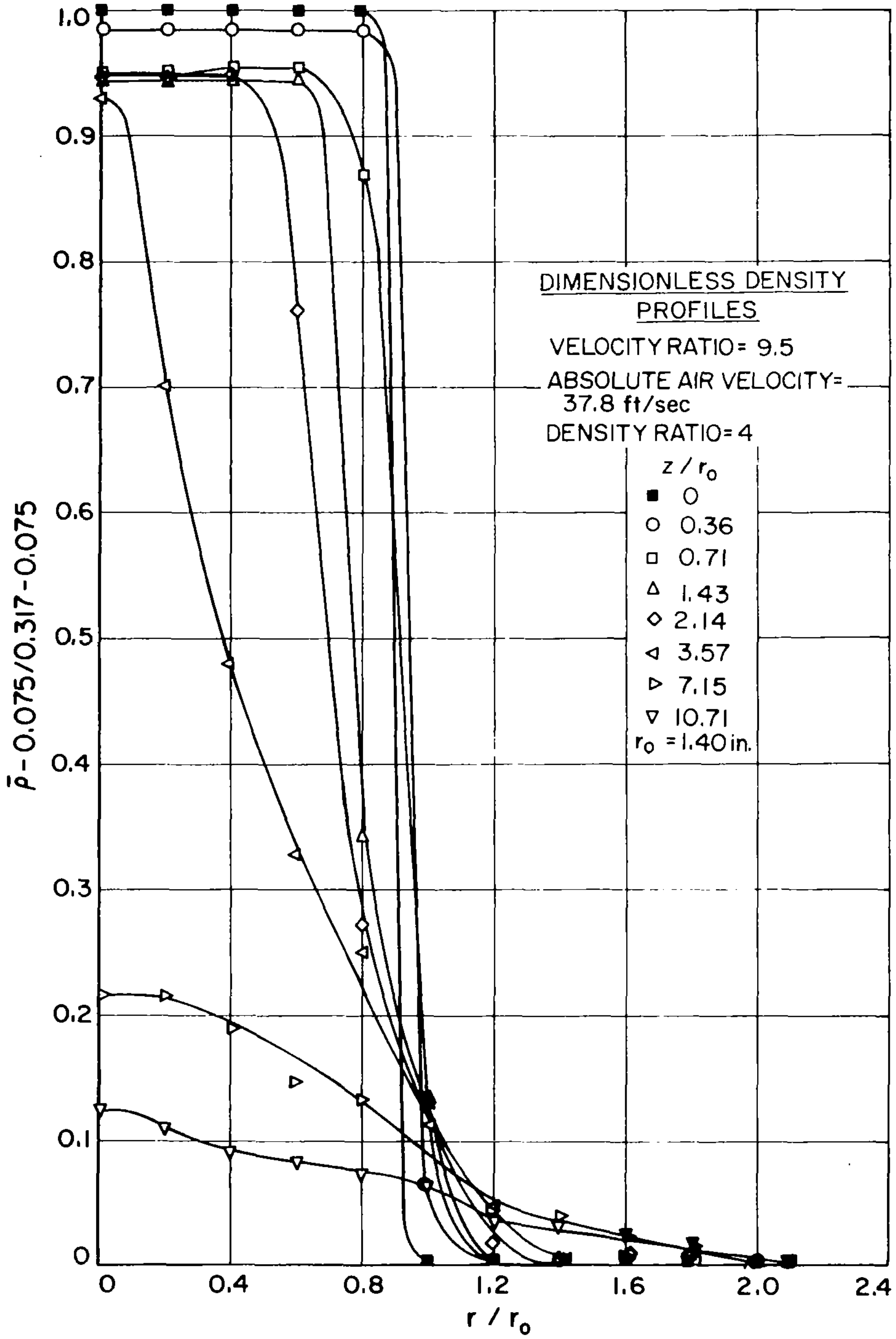

DIMENSIONLESS DENSITY PROFILES
VELOCITY RATIO= 9.5
ABSOLUTE AIR VELOCITY= 37.8 ft/sec
DENSITY RATIO= 4
z/r_0
■ 0
○ 0.36
□ 0.71
△ 1.43
◇ 2.14
◁ 3.57
▷ 7.15
▽ 10.71
r_0 = 1.40 in.
$\bar{\rho}$-0.075/0.317-0.075
1.0
0.9
0.8
0.7
0.6
0.5
0.4
0.3
0.2
0.1
0
0
0.4
0.8
1.2
1.6
2.0
2.4
r/r_0

FIGURE 18

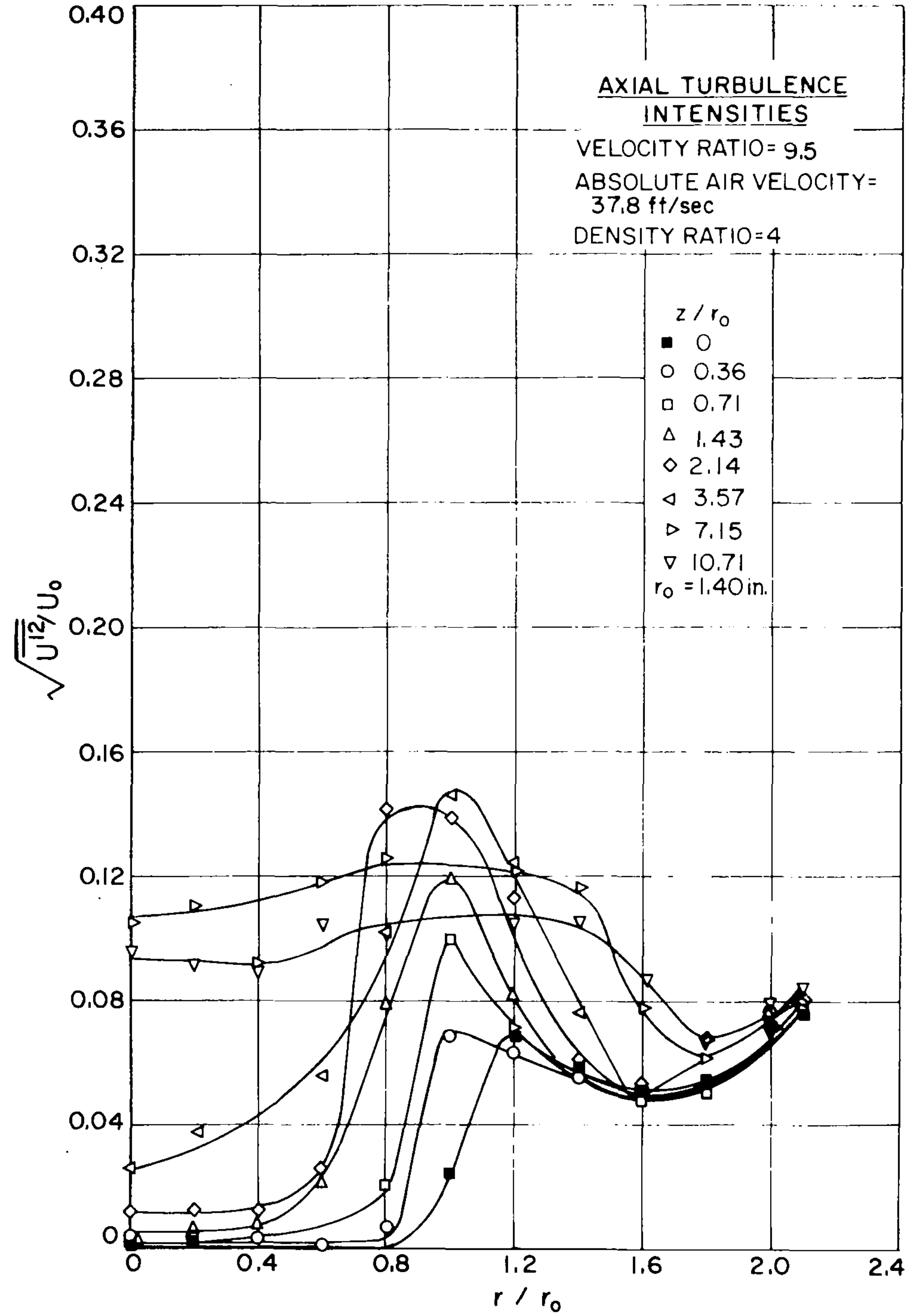
AXIAL TURBULENCE INTENSITIES
VELOCITY RATIO= 9.5
ABSOLUTE AIR VELOCITY= 37.8 ft/sec
DENSITY RATIO=4
z / r_o
■ 0
○ 0.36
□ 0.71
△ 1.43
◇ 2.14
◁ 3.57
▷ 7.15
▽ 10.71
r_o =1.40 in.
$\sqrt{\overline{u'^2}}/U_o$
0.40
0.36
0.32
0.28
0.24
0.20
0.16
0.12
0.08
0.04
0
0.4
0.8
1.2
1.6
2.0
2.4
r / r_o

FIGURE 19

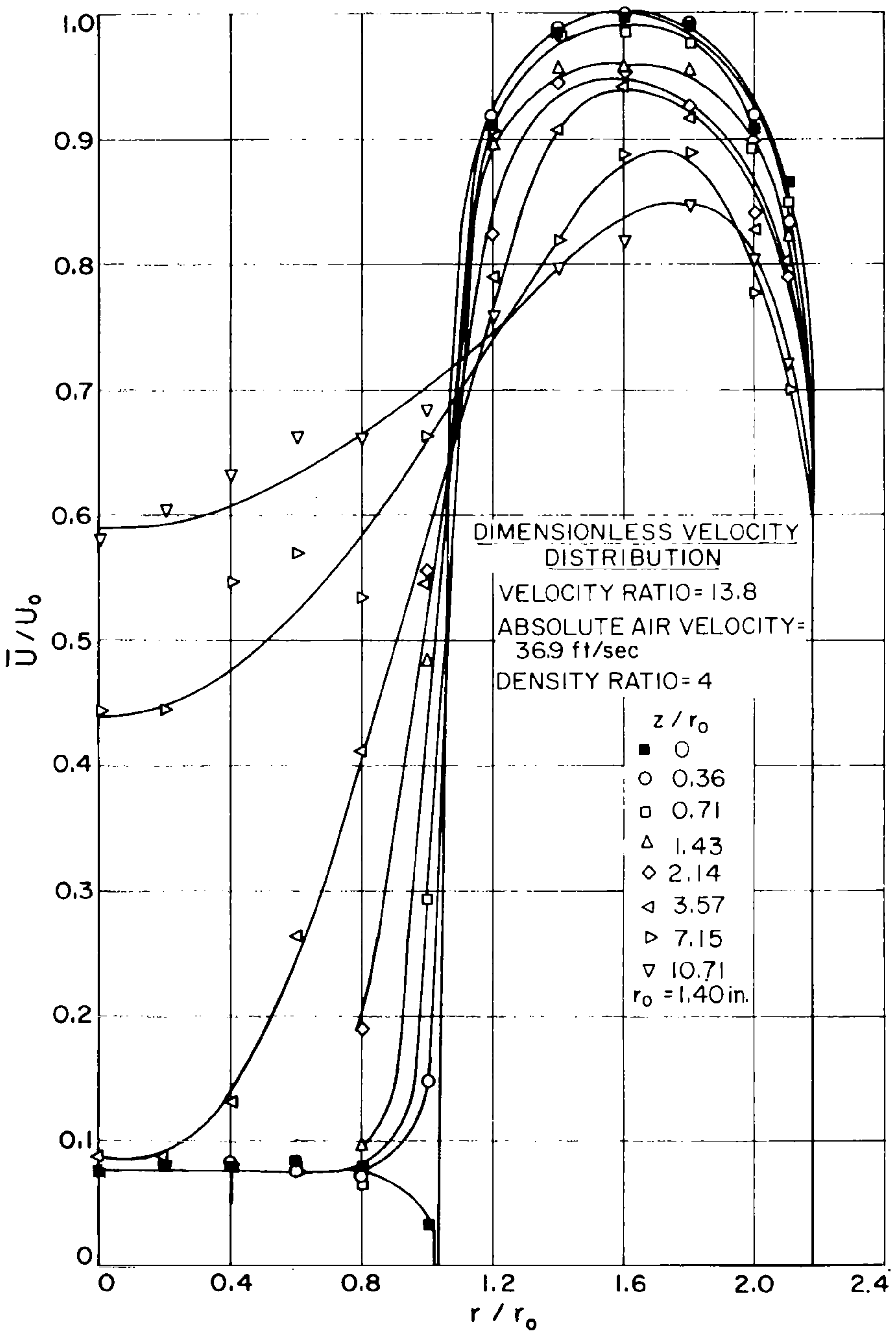
DIMENSIONLESS VELOCITY DISTRIBUTION
VELOCITY RATIO= 13.8
ABSOLUTE AIR VELOCITY= 36.9 ft/sec
DENSITY RATIO= 4
z / r_o
■ 0
○ 0.36
□ 0.71
△ 1.43
◇ 2.14
◁ 3.57
▷ 7.15
▽ 10.71
r_o = 1.40 in.
$\bar{U} / U_o$
0
0.1
0.2
0.3
0.4
0.5
0.6
0.7
0.8
0.9
1.0
r / r_o
0
0.4
0.8
1.2
1.6
2.0
2.4

FIGURE 20

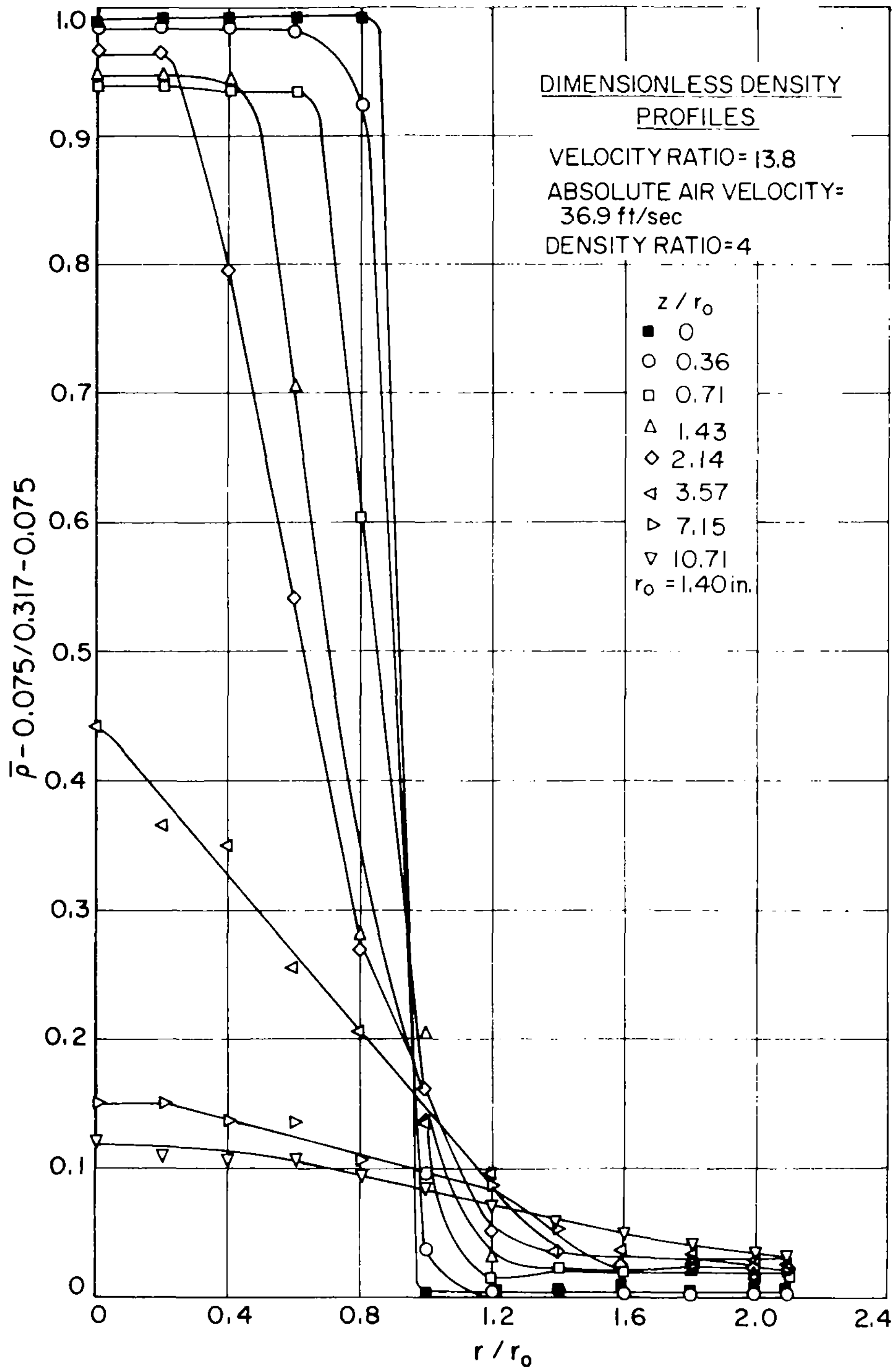DIMENSIONLESS DENSITY PROFILES
VELOCITY RATIO = 13.8
ABSOLUTE AIR VELOCITY = 36.9 ft/sec
DENSITY RATIO = 4
z/r_0
■ 0
○ 0.36
□ 0.71
△ 1.43
◇ 2.14
◁ 3.57
▷ 7.15
▽ 10.71
r_0 = 1.40 in.
$\bar{\rho}-0.075/0.317-0.075$
1.0
0.9
0.8
0.7
0.6
0.5
0.4
0.3
0.2
0.1
0
0
0.4
0.8
1.2
1.6
2.0
2.4
r/r_0

FIGURE 21

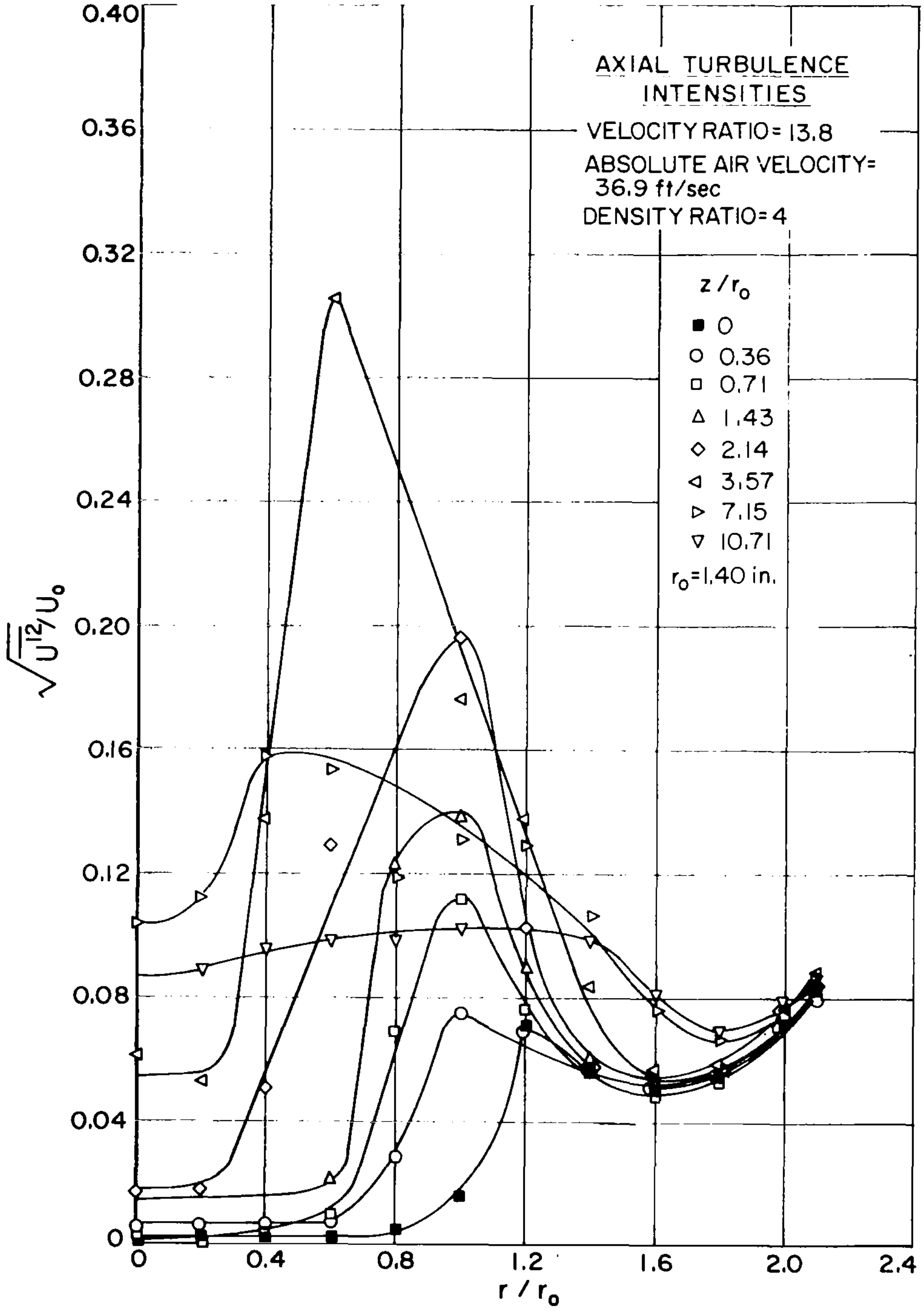
AXIAL TURBULENCE INTENSITIES
VELOCITY RATIO = 13.8
ABSOLUTE AIR VELOCITY = 36.9 ft/sec
DENSITY RATIO = 4
z/r_o
■ 0
○ 0.36
□ 0.71
△ 1.43
◇ 2.14
◁ 3.57
▷ 7.15
▽ 10.71
r_o=1.40 in.
$\sqrt{\overline{u'^2}}/U_o$
0.40
0.36
0.32
0.28
0.24
0.20
0.16
0.12
0.08
0.04
0
0
0.4
0.8
1.2
1.6
2.0
2.4
r/r_o

FIGURE 22

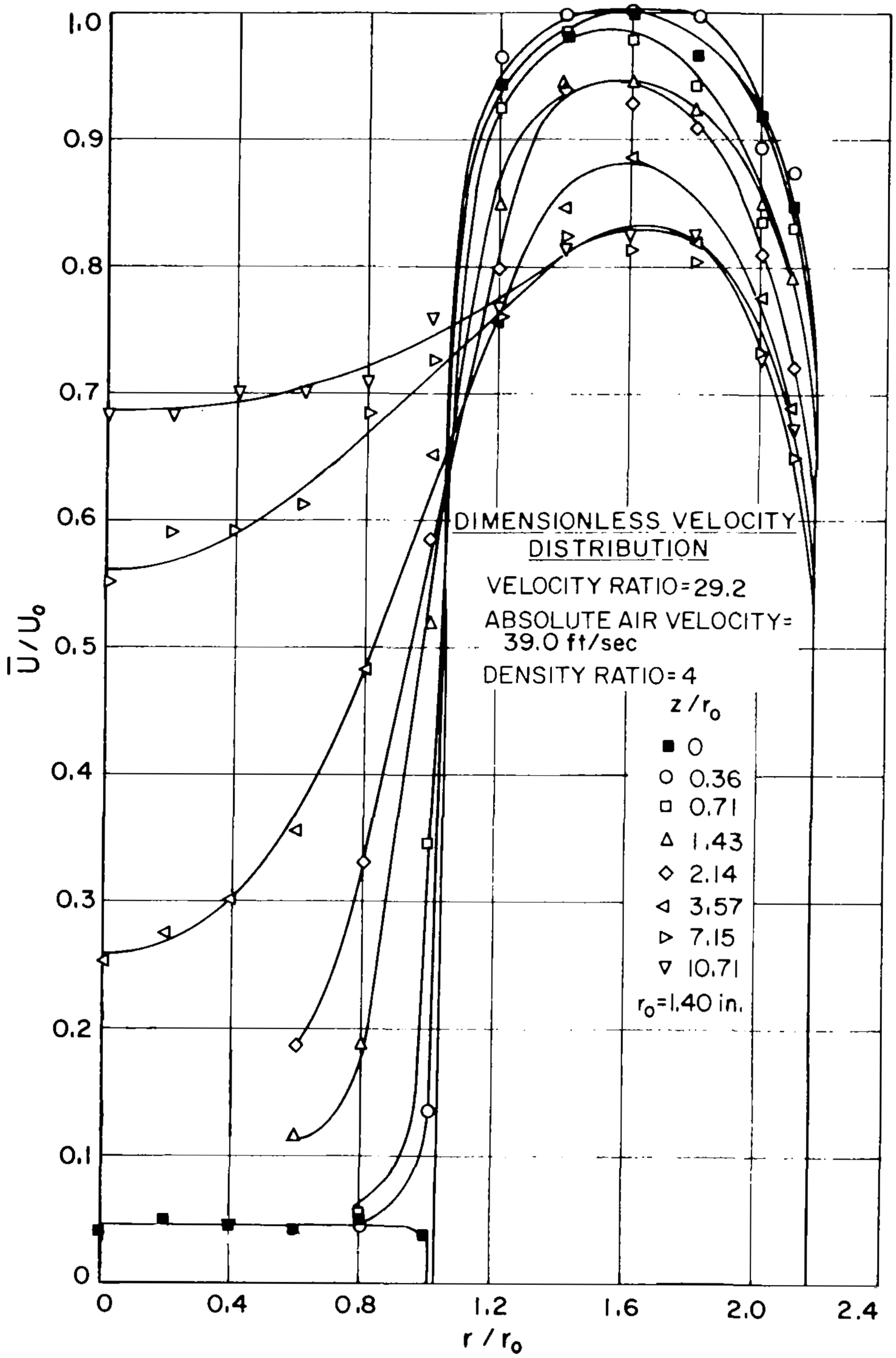
DIMENSIONLESS VELOCITY DISTRIBUTION
VELOCITY RATIO=29.2
ABSOLUTE AIR VELOCITY= 39.0 ft/sec
DENSITY RATIO=4
z/r_0
■ 0
○ 0.36
□ 0.71
△ 1.43
◇ 2.14
◁ 3.57
▷ 7.15
▽ 10.71
r_0=1.40 in.
$\overline{U}/U_0$
1.0
0.9
0.8
0.7
0.6
0.5
0.4
0.3
0.2
0.1
0
0
0.4
0.8
1.2
1.6
2.0
2.4
r/r_0

FIGURE 23

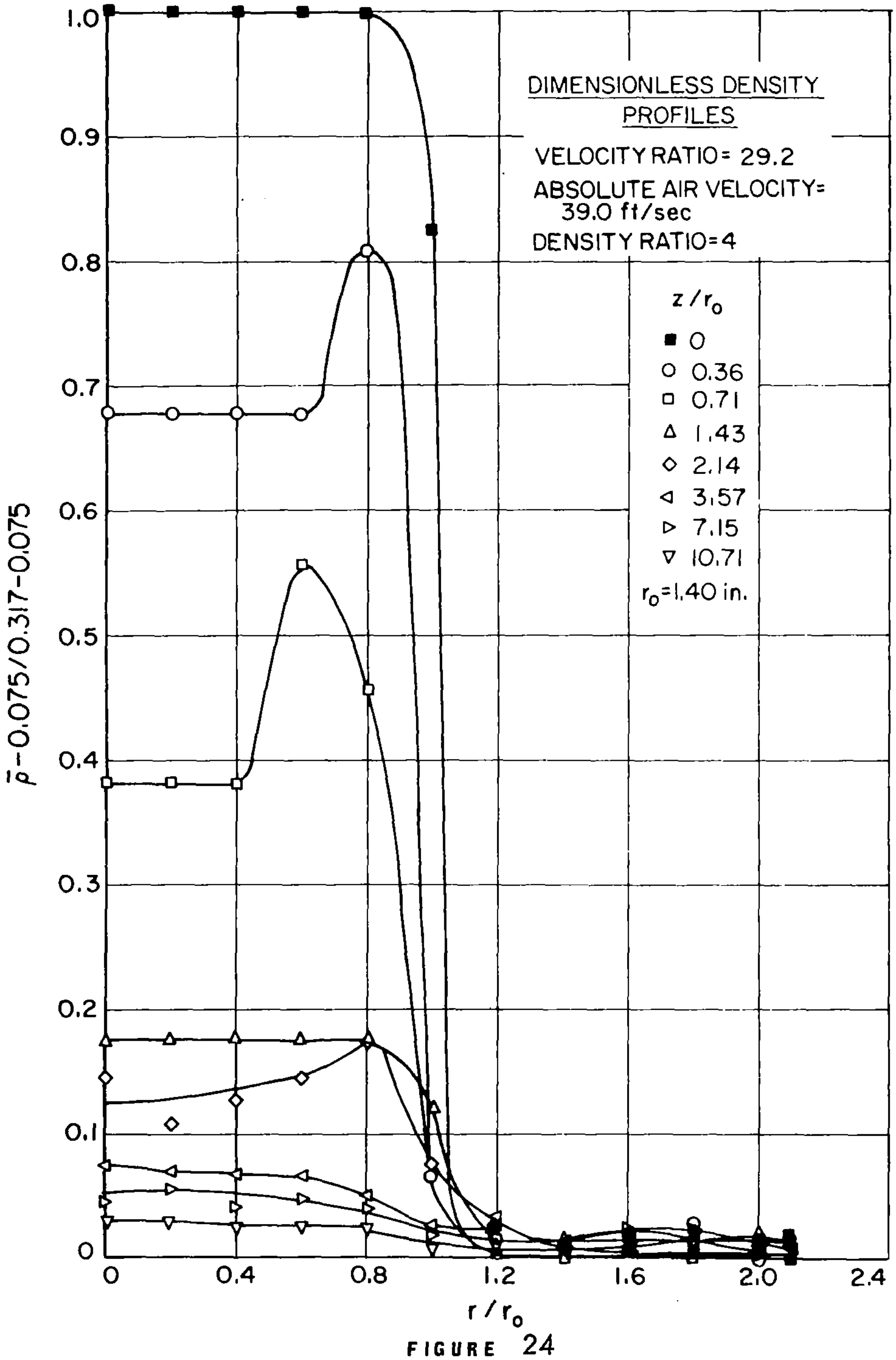
DIMENSIONLESS DENSITY PROFILES
VELOCITY RATIO= 29.2
ABSOLUTE AIR VELOCITY= 39.0 ft/sec
DENSITY RATIO=4
z/r_o
■ 0
○ 0.36
□ 0.71
△ 1.43
◇ 2.14
◁ 3.57
▷ 7.15
▽ 10.71
r_o=1.40 in.
$\bar{\rho}$-0.075/0.317-0.075
1.0
0.9
0.8
0.7
0.6
0.5
0.4
0.3
0.2
0.1
0
0
0.4
0.8
1.2
1.6
2.0
2.4
r/r_o

FIGURE 24

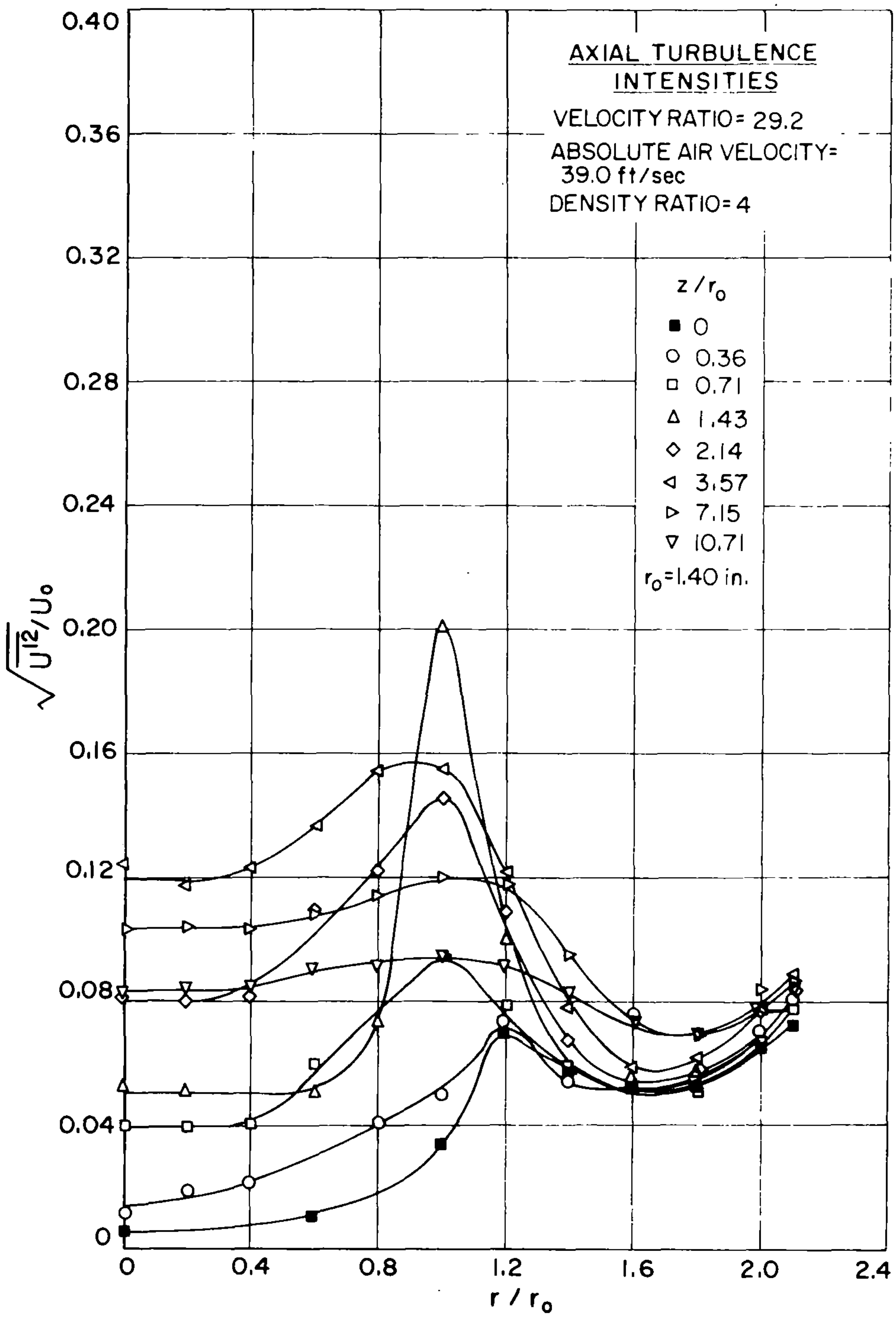
AXIAL TURBULENCE INTENSITIES
VELOCITY RATIO= 29.2
ABSOLUTE AIR VELOCITY= 39.0 ft/sec
DENSITY RATIO= 4
z/r_o
■ 0
○ 0.36
□ 0.71
△ 1.43
◇ 2.14
◁ 3.57
▷ 7.15
▽ 10.71
r_o=1.40 in.
$\sqrt{\overline{u'^2}}/U_o$
0.40
0.36
0.32
0.28
0.24
0.20
0.16
0.12
0.08
0.04
0
0
0.4
0.8
1.2
1.6
2.0
2.4
r/r_o

FIGURE 25

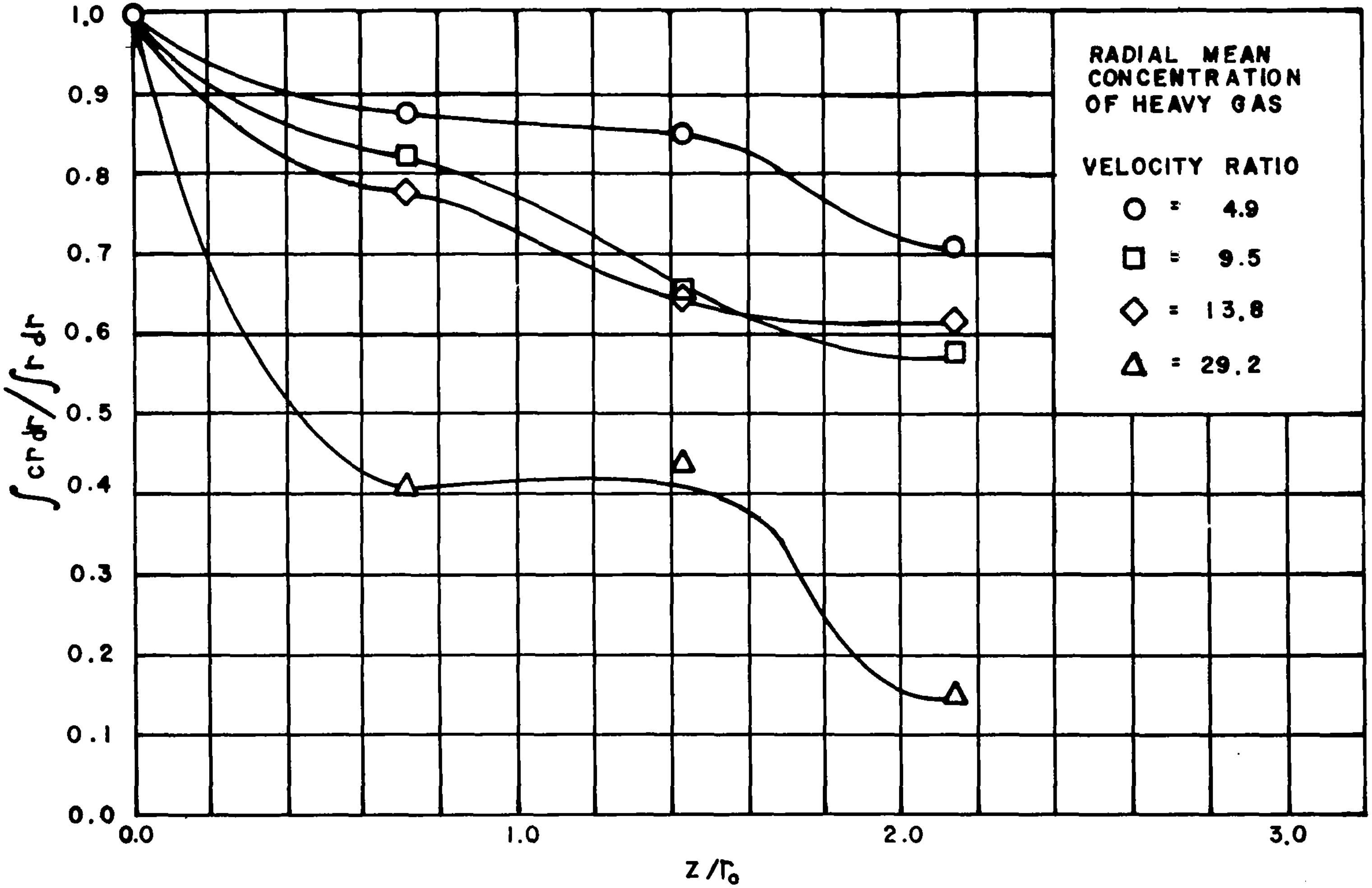

MASS HOLDUP FIGURE 26

simultaneously. The last profile taken at a velocity ratio of 29.2 indicates a wake back-flow type of behavior. The amount of Freon at the tube exit is probably lower than the indicated 1.0 due to backmixing. The concentration is seen to rise to a local maximum indicating a standing circulation pattern. The final decrease in Freon concentration is due to the breakup and mixing in the wake behind the circulation pattern.

CONCLUSIONS

1. The suggestion by Zawacki that the problem of unbounded coaxial flow is one of combined wake-coaxial flow with possible backflow is supported for confined coaxial flow by the results of this work in both the homogeneous and heterogeneous cases. At high velocity ratios, the wake flow predominates. High fluctuations and flow patterns of an undetermined nature occur.

2. The shapes of the axial turbulence intensity profiles are similar for both homogeneous and heterogeneous cases but the homogeneous intensities is somewhat larger in magnitude.

3. For the homogeneous case, radial turbulence intensity profiles were similar in shape to the axial turbulence intensity curves. However, the ratio of axial turbulence intensity to radial turbulence intensity is approximately 1.5, the same as for unbounded coaxial flow.

4. The higher density Freon caused a decrease in momentum transfer and a preservation of the inner stream as compared to the homogeneous case.

5. The presence of a concentration potential core was found, and the length of this pure Freon core was shown to depend on the velocity ratio; the higher the velocity ratio, the shorter the core.

BIBLIOGRAPHY

1. Prandtl, L., "Bericht Uber Untersuchunger zer Ausgebildeten Turbulenz", Zamm 5, 136, 1925.

2. Prandtl, L., "Bemerkung zur Theories der Freien Turbulenz", Zamm 22, 5, 1942.

3. Taylor, G. I., "The Transport of Vorticity and Heat Through Fluids in Turbulent Motion", Proc. Roy. Soc., London, A135, 685, 1932.

4. Reichardt, H., "Gesetmassigkeiten der Freien Turbulenz", VDI-Forschungsh, 414, 1951.

5. Keuthe, A. M., "Investigation of the Turbulent Region Formed by Jets", Journal of Applied Mechics, Trans. ASME Vol. 57, 1935.

6. Tollmien, W., "Berechnung Turbulenter Aus Breitungsvorgange", Zamm 6, 1926 Translated as NACA TM 1085, 1945.

7. Goertler, H., "Berechnung von Aufgaben der Freien Turbulenz auf Grund eines neuen Naherungsansatzes", Zamm 22, 1942.

8. Squire, H. B., and Trouncer, J. "Round Jets in a General Stream". Aeronnautical Research Committee Tech. Report R and M No. 1974, 1944.

9. Torda, T. P., and Stillwell, H. S., Analytical and Experimental Investigations of Incompressible and Compressible Mixing of Streams and Jets, Wright Air Development Center, TR 55- 337, 1956.

10. Torda, T. P., Thompson, W. J., and Genetti, B. K., "Laminar Incompressible Mixing of Two-dimensional and Axially Symmetric Jets", Proceedings of the Second U.S. Congress of Applied Mechanics, 465, 1951.

11. Liepmann, H. W. and Laufer, J., "Investigations of Free Turbulent Mixing", NACA TN 1257, 1947.

12. Forstall, W. Jr. and Shapiro, A. H., "Momentum and Mass Transfer in Coaxial Jets", Journal of Applied Mechanics, Vol. 17, No. 12, 399, 1950.

13. Corrsin, S. and Uberoi, M. S., "Further Experiments in the Flow and Heat Transfer in a Heated Turbulent Jet", NACA Report 998, 1950.

14. Kobashi, Y. and Tani, I., "Experimental Studies on Compound Jets", Proceedings of the Second Japan National Congress for Applied Mechanics, 465, 1951.

15. Conger, W. L., "Measurement of Concentration Fluctuations in the Mixing of Two Gases by Hot Wire Anemometer Techniques", Ph. D. Thesis, Univ. of Penn., 1965.

16. Rosenweig, R. E., "Measurement and Characterization of Turbulent Mixing", Fuels Research Laboratory, 1959.

17. Blackshear, P. L. Jr. and Fingerson, L., "Rapid Response Heat Flux Probe for High Temperature Gases", ARS Journal, 1962.

18. Alpinieri, L. J., "An Experimental Investigation of the Turbulent Mixing of Non-homogeneous Coaxial Jets", Polytechnic Institute of Brooklyn, PIBAL Report 789, 1963; also "Turbulent Mixing of Coaxial Jets", AIAA Journal, Vol. 2, 1560, 1964.

19. Boehman, L., "Mass and Momentum Transport Properties in Isoenergetic Coaxial Flows", Ph. D. Thesis, Ill. Inst. of Tech., 1967

20. Zawacki, T., "Turbulence in the Mixing Region of Coaxial Streams", Ph. D. Thesis, Ill. Inst. of Tech., 1967.

21. D'souza, G. J., "Turbulent Correlations in a Coaxial Flow of Dissimilar Fluids", M. S. Thesis, Ill. Inst. of Tech., 1967.

22. Hill, P. G., "Turbulent Jets in Ducted Streams", J.F.M., Vol. 22, 161, 1965.

23. Curtet, R., "Confined Jets and Reciruclation Phenomenon With Cold Air", Combustion and Flame, 1958.

24. Curtet, R. and Ricou, "On the Tendency to Self-Preservation in Axisymmetric Ducted Jets", Journal of Basic Engineering, 1964.

25. King, L. V., Phil. Trans. Roy. Soc. London, 214A, 273, 1917.

26. Johnson, Bruce V., and Clark, James W., Multi-Component Coaxial Flow J t Jets in Short Chambers", United Aircraft Research Laboratories Report G G 910091-16, April, 1968.

27. Corrsin, S., "Extended Applications of the Hot Wire Anemometer", NACA Technical Note 1864, 1949.

28. Montealegre, A. P., "Evaluations of Turbulent Correlations in a Coaxial Flow", M. S. Thesis, Ill. Inst. of Tech., 1967.